U.S. Department of Transportation

Federal Railroad Administration

Assessment of Rail Seat Abrasion Patterns and Environment

Office of Railroad
Policy and Development
Washington, DC 20590

DOT/FRA/ORD-12/07

Final Report
May 2012

REPORT DOCUMENTATION PAGE

Form Approved
OMB No. 0704-0188

1. AGENCY USE ONLY (Leave blank)	2. REPORT DATE	3. REPORT TYPE AND DATES COVERED
	May 2012	Technical Report

4. TITLE AND SUBTITLE
Assessment of Rail Seat Abrasion Patterns and Environment

5. FUNDING NUMBERS
DTFR53-00-C-00012
Task Order 246

6. AUTHOR(S) and FRA COTR
Richard Reiff, Russell Walker, Patricia Schreiber, Nicholas Wilson, and Hugh Thompson

7. PERFORMING ORGANIZATION NAME(S) AND ADDRESS(ES)
Transportation Technology Center, Inc.
55500 DOT Road
Pueblo, CO 81001

8. PERFORMING ORGANIZATION REPORT NUMBER

9. SPONSORING/MONITORING AGENCY NAME(S) AND ADDRESS(ES)
U.S. Department of Transportation
Federal Railroad Administration
Office of Railroad Policy and Development
Washington, DC 20590

10. SPONSORING/MONITORING AGENCY REPORT NUMBER
DOT/FRA/ORD-12/07

11. SUPPLEMENTARY NOTES
Program Manager: Hugh Thompson

12a. DISTRIBUTION/AVAILABILITY STATEMENT
This document is available to the public through the FRA Web site at http://www.fra.dot.gov.

12b. DISTRIBUTION CODE

13. ABSTRACT (Maximum 200 words)
Rail seat abrasion (RSA) of concrete ties is manifested by the loss of material under the rail seat area and, in extreme cases, results in loss of rail clip holding power, reverse rail cant, and gauge widening. RSA was measured in several curves on two railroads. The measurements encompass a range of environmental conditions and track curvature. The RSA measurements, track geometry measurements, and wheel/rail forces predicted with NUCARS® were compared to identify a correlation between wheel/rail forces and deep, wedge-shaped abrasion. RSA and wheel/rail forces were found to be related to curvature, but no clear examples were found where rail forces and RSA could be correlated to a local track geometry deviation. Comparisons were hampered by cases where RSA was measured in locations where previous repairs had been made and by other cases where very little RSA was present at the sites measured.

14. SUBJECT TERMS
Rail seat abrasion, concrete ties

15. NUMBER OF PAGES
59

16. PRICE CODE

17. SECURITY CLASSIFICATION OF REPORT	18. SECURITY CLASSIFICATION OF THIS PAGE	19. SECURITY CLASSIFICATION OF ABSTRACT	20. LIMITATION OF ABSTRACT
Unclassified	Unclassified	Unclassified	

NSN 7540-01-280-5500
Standard Form 298 (Rev. 2-89)
Prescribed by ANSI Std. 239-18
298-102

METRIC/ENGLISH CONVERSION FACTORS

ENGLISH TO METRIC	METRIC TO ENGLISH
LENGTH (APPROXIMATE)	**LENGTH (APPROXIMATE)**
1 inch (in) = 2.5 centimeters (cm)	1 millimeter (mm) = 0.04 inch (in)
1 foot (ft) = 30 centimeters (cm)	1 centimeter (cm) = 0.4 inch (in)
1 yard (yd) = 0.9 meter (m)	1 meter (m) = 3.3 feet (ft)
1 mile (mi) = 1.6 kilometers (km)	1 meter (m) = 1.1 yards (yd)
	1 kilometer (km) = 0.6 mile (mi)
AREA (APPROXIMATE)	**AREA (APPROXIMATE)**
1 square inch (sq in, in^2) = 6.5 square centimeters (cm^2)	1 square centimeter (cm^2) = 0.16 square inch (sq in, in^2)
1 square foot (sq ft, ft^2) = 0.09 square meter (m^2)	1 square meter (m^2) = 1.2 square yards (sq yd, yd^2)
1 square yard (sq yd, yd^2) = 0.8 square meter (m^2)	1 square kilometer (km^2) = 0.4 square mile (sq mi, mi^2)
1 square mile (sq mi, mi^2) = 2.6 square kilometers (km^2)	10,000 square meters (m^2) = 1 hectare (ha) = 2.5 acres
1 acre = 0.4 hectare (he) = 4,000 square meters (m^2)	
MASS - WEIGHT (APPROXIMATE)	**MASS - WEIGHT (APPROXIMATE)**
1 ounce (oz) = 28 grams (gm)	1 gram (gm) = 0.036 ounce (oz)
1 pound (lb) = 0.45 kilogram (kg)	1 kilogram (kg) = 2.2 pounds (lb)
1 short ton = 2,000 pounds (lb) = 0.9 tonne (t)	1 tonne (t) = 1,000 kilograms (kg) = 1.1 short tons
VOLUME (APPROXIMATE)	**VOLUME (APPROXIMATE)**
1 teaspoon (tsp) = 5 milliliters (ml)	1 milliliter (ml) = 0.03 fluid ounce (fl oz)
1 tablespoon (tbsp) = 15 milliliters (ml)	1 liter (l) = 2.1 pints (pt)
1 fluid ounce (fl oz) = 30 milliliters (ml)	1 liter (l) = 1.06 quarts (qt)
1 cup (c) = 0.24 liter (l)	1 liter (l) = 0.26 gallon (gal)
1 pint (pt) = 0.47 liter (l)	
1 quart (qt) = 0.96 liter (l)	
1 gallon (gal) = 3.8 liters (l)	
1 cubic foot (cu ft, ft^3) = 0.03 cubic meter (m^3)	1 cubic meter (m^3) = 36 cubic feet (cu ft, ft^3)
1 cubic yard (cu yd, yd^3) = 0.76 cubic meter (m^3)	1 cubic meter (m^3) = 1.3 cubic yards (cu yd, yd^3)
TEMPERATURE (EXACT)	**TEMPERATURE (EXACT)**
[(x-32)(5/9)] °F = y °C	[(9/5) y + 32] °C = x °F

QUICK INCH - CENTIMETER LENGTH CONVERSION

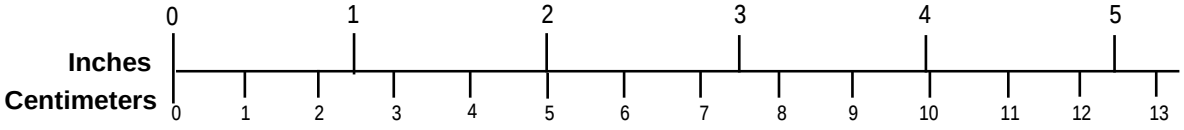

QUICK FAHRENHEIT - CELSIUS TEMPERATURE CONVERSION

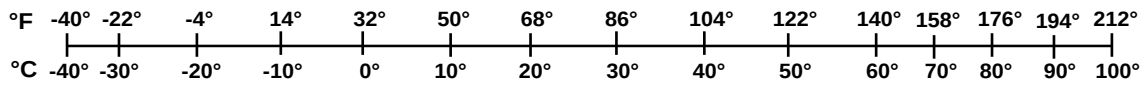

For more exact and or other conversion factors, see NIST Miscellaneous Publication 286, Units of Weights and Measures. Price $2.50 SD Catalog No. C13 10286

Updated 6/17/98

Acknowledgments

TTCI would like to acknowledge the support provided by the following people for this project: Mike Coltman, John A. Volpe National Transportation Systems Center (Volpe Center); Brian Marquis, Volpe Center; John Choros, Volpe Center; Seth Ogan, BNSF Railway; Mark Austin, CSX; and Hugh Thompson, Federal Railroad Administration, Office of Railroad Policy and Development.

Contents

Illustrations

Tables

Executive Summary

Rail seat abrasion (RSA) of concrete ties is manifested by the loss of material under the rail seat area and, in extreme cases, results in loss of rail clip holding power, reverse rail cant, and gauge widening. RSA was found to be related to the average forces created by track curvature. RSA could not be correlated to a localized track geometry feature in the measurements made as part of this research program.

The objective of this project was to identify the field conditions where RSA is occurring. Ideally, the measurements would have identified localized areas of deep, wedge-shaped abrasions that contribute to loss of rail cant and gauge widening, and then, it would have documented the track geometry and wheel/rail force environment that led to such a condition. These results might have been used to design a modification to a short section of the Facility for Accelerated Service Testing (FAST) High Tonnage Loop at the Transportation Technology Center (TTC) near Pueblo, CO, to induce high wheel/rail forces for the purpose of monitoring RSA growth.

RSA was inspected and measured in 16 curves on two railroads, encompassing a range of environmental conditions and track curvature. For a few of the measured curves, RSA measurements were compared with measured track geometry and wheel/rail forces generated by NUCARS®[1] simulations to correlate wheel/rail forces and abrasion depth. The NUCARS simulations confirmed the correlation of RSA with track curvature but could not identify local track geometry features associated with severe RSA. To more clearly differentiate specific features, more accurate input to the NUCARS simulations related to the specific site may be required such as rail lubrication, types of vehicles running over the site, and variations in the rail fastener and support conditions. The St. Albans, WV, sites had the tightest curvature, the highest annual precipitation, and the deepest RSA. Many of the curves at this location had previous repairs. It was impossible to determine whether the measured abrasion was recent or present at the time of previous repair, because the previous repair material was often removed as part of the pad removal and seat cleaning process.

The Needles, CA, sites had the next tightest curvature and the least annual precipitation. These curves had not been previously repaired. Only one of the curves measured had measureable RSA. This was just the onset of abrasion, and it was occurring along the gauge side of the rail seat.

The Alliance, NE, site had the lowest curvature, and its precipitation levels were between those of Needles and St. Albans, although much closer to Needles. Some of the curves had been repaired previously and some had not. The Alliance curves showed very little abrasion.

RSA measurements required rail removal; therefore, the inspections were coordinated with the cooperating railroads' rail replacement or rail seat repair schedules. Measurements were contingent on not interfering with the repair teams and allowed very limited time for RSA measurement. Most measurements were made with a steel template and a digital depth gauge, although a prototype automated measurement system was tried. For future work, an improved automated device is recommended to allow more measurements in the limited time available.

[1] NUCARS® is a registered trademark of Transportation Technology Center, Inc.

1. Introduction

RSA of concrete ties is manifested by the loss of material under the rail seat area and reduction of rail clip holding power. This condition, especially at its onset, is difficult to detect visually. Severe abrasion can result in loss of clip toe load, rail tipping (cant), and wide gauge and can cause derailment. Figure 1 shows an example of severe RSA.

Figure 1. Example of Severe RSA

Several programs sponsored by the railroad industry, suppliers, and FRA are in place to develop RSA detection systems; however, to solve the problem, the root cause must be determined. RSA is known to occur in areas of high loads, sharp curves, and high precipitation. However, because RSA does not occur everywhere, one theory suggests that selected combinations of track geometry track fastener and support conditions, and other local and environmental conditions result in increased wheel/rail forces that are incipient to the damaging conditions that result in RSA.

The work under this phase of the project assessed field conditions where RSA was reported to be occurring and produced comparisons of wheel/rail forces and track forces on the basis of predicted vehicle dynamic response to track geometry inputs. These results are intended to provide input for developing a predictive model for RSA detection.

1.1 Background

Detailed track inspection at the locations of two derailments attributed to RSA indicated concrete ties exhibited an excessively large wedge shaped loss of material on the field side of the rail seat area. At these locations, loss of material was present for a short portion of a curve corresponding to a track location that contained a “down and out” geometry irregularity on the outside rail of the curve. The John A. Volpe National Transportation Systems Center (Volpe) conducted analyses that estimated that the combination of the vertical and lateral wheel forces resulting

from these types of track geometry irregularities can result in rail base field side stresses exceeding the design compression capacity of concrete ties [1].

The objective of this research project was to explore the correlation between development of the wedge-shaped form of RSA and dynamic wheel/rail interaction loads resulting in field side pressures in excess of typical concrete strength and how these loads relate to initiation and growth of this type of RSA.

Development of RSA has previously been studied at the FAST High Tonnage Loop at TTC, but did not focus on the effects of particular track geometry features [2, 3]. The previous research evaluated the performance of new and different rail fastener and rail seat components and materials for their effects on reducing rail RSA. Different methods for repairing RSA were also evaluated.

The scope of this project was divided into two major segments. The first segment (subject of this report) investigated RSA found in track under revenue service conditions and compared it to measured track geometry to determine whether the hypothesized deviations suspected to result in high applied concrete surface stress correlated to field RSA measurements. The intent of this investigation was to characterize the types of RSA occurring in revenue service, and where located, to identify the conditions, which may contribute to the occurrence of wedge-shaped abrasions.

The second, follow-on segment in 2012 is planned to develop experiments that, under a controlled environment, will produce conditions necessary for the initiation and growth of this type of RSA. The second segment is also expected to complete the development of the predictive model, which builds on field assessment results. This work would also include field validation of track segments where the model predictions show no occurrence of RSA. In addition, on the basis of predictive modeling and track test results, future deliverables would include development of best practices to reduce the tendency of RSA. Modeling development and associated efforts will be conducted primarily by the engineering staff from Volpe, while field assessment and activity coordination will be the primary responsibility of Transportation Technology Center, Inc. (TTCI).

1.2 Project Objectives

The first segment of the project had three main objectives:

- Measure RSA at selected revenue service sites to determine severity and extent of RSA, depth and patterns of RSA, and track geometry.
- Use the field measurements as input to NUCARS simulations to determine track features and locations where vehicle performance was expected to introduce high lateral loads into the track.
- Use the results of the measurements and NUCARS simulations to identify potential track geometry features for use in a future project for modifying a short segment of the FAST High Tonnage Loop to purposely induce high truck side lateral/vertical (L/V) ratios for monitoring the effect on developing RSA and/or track component damage.

Concurrently, survey measurements and simulation results were provided to the Federal Railroad Administration (FRA) and Volpe to support their efforts in developing RSA

predictive modeling tools. Using this information, Volpe engineering staff will lead the effort to determine whether common vehicle track interaction characteristics can be reliably used to accurately predict development, growth, and severity of RSA.

2. Project Method

For the first segment of work, TTCI developed detailed test plans for field inspection and measurement. These were reviewed by Hugh Thompson (FRA Contracting Officer's Technical Representative - COTR) and Volpe engineering staff to ensure that the data obtained, addressed future requirements of the planned modeling effort. A technical advisory group (TAG) was established to coordinate the two participating railroads (CSX and BNSF Railway (BNSF)). To address their specific needs, each railroad assigned a track engineer to help coordinate field inspections and provide track geometry measurements for use in subsequent analyses. This included obtaining work plans, traffic history, track geometry history, and ensuring safe and legal track access to obtain measurements.

2.1 Field Survey and Measurement Approach

To obtain field data, a significant effort was required by personnel from the cooperating railroads to provide access to locations on track, track inspection data, and historical information. Because no acceptable or validated means of measuring RSA depth and shape with rail in place currently exists, the field measurements required access to rail seats during periods when the railroads were changing rail and/or repairing rail seats. Examples of this situation are shown in Figure 2 and Figure 3 (ties reported to have RSA but with rail still attached). Figure 4 is the same approximate location but with the rail removed, showing variations in RSA over just a few ties. Note that the large tie plates shown in these photographs were installed to mitigate and control RSA at these particular locations.

Figure 2. Example of Ties Reported to Have RSA, but with Rail in Place It Is not Feasible to Measure RSA Depth
(New replacement rail pads are in ballast next to ties in preparation of RSA repair.)

Figure 3. Another View of the Same General Location as Shown in Figure 2; Ties Reported to Have RSA, but with Rail in Place It Is not Feasible to Measure RSA Depth

Figure 4. Example of Ties Shown in Figures 2 and 3 with Rail Removed, Showing Depth of RSA

(Note that RSA depth is not uniform from tie to tie. The red arrows show that the two nearest ties have RSA undercutting the fastener clip, whereas the green arrow shows that the third tie has much less RSA and no undercutting.)

Because the rail blocks the ability to measure depth, locations where RSA data could be collected were contingent on when and where rail removal work was planned by the participating railroads. In many cases, last-minute issues and emerging conditions such as track time, equipment delays, and availability of railroad personnel limited the data that could be collected.

For each area or subdivision where RSA was suspected based on aging track conditions, the work plan for the host railroad was provided. Curves were compared to track chart data and a prework inspection conducted to assess site conditions. This included walking each curve, locating key curve points including points of tangent to spiral, spiral to curve, curve to spiral and spiral to tangent. A tie numbering system was established at each curve associated with a nearby feature such as a milepost (MP) marker. This method was selected over detailed distance measurements, because ties are on 2.0-foot centers, and by counting tie numbers an accurate distance could be determined for any specific location. Ties were numbered by marking every tenth tie in the planned direction of work (Ties 0, 10, 20, etc.) to facilitate correlating location with RSA data collected during the maintenance activity. Where such inspections could be conducted well in advance of the actual track work, the cross section profiles on both rails were measured by using a MiniProf™ profilometer at the key curve points (above) and at several locations within the full body of the curve. Other notes were made on localized site variations and conditions that might contribute to variable loading, such as low spots, alignment kinks, etc. The speed and type of train traffic normally operated over the sites was observed, and details were provided by the host railroads. Any other parameters identified as being important to the formation of RSA were also noted. However, in the short windows of time allowed there was not sufficient time to collect detailed information about the condition of specific fastener components: clips, insulators, and pads.

Either before or after the inspection, the most recent track geometry data (prior to planned work) was obtained for comparison with the RSA data and for use in the NUCARS vehicle dynamic performance predictions.

To aid in RSA depth and shape measurements, TTCI fabricated a prototype laser trace fixture that measures the RSA depth around the edge of the rail seat, as Figure 5 shows.

Figure 5. Automated RSA Profile Data Collection System Prototype Used to Collect the Perimeter Depth and Pattern of RSA

The automated laser device was a prototype and was not sufficiently robust to withstand field test environments and handling. Rain or moisture easily damaged controls and electrical systems, and it was too cumbersome to rapidly collect data. In addition, the large size and relatively small triangular-shaped base of the machine led to problems, because it tipped during the measurement process and created data errors. To supplement the automated system, manual measurements were utilized by using a flat template and dial indicator gauge. Figure 6 shows the template used in the manual system.

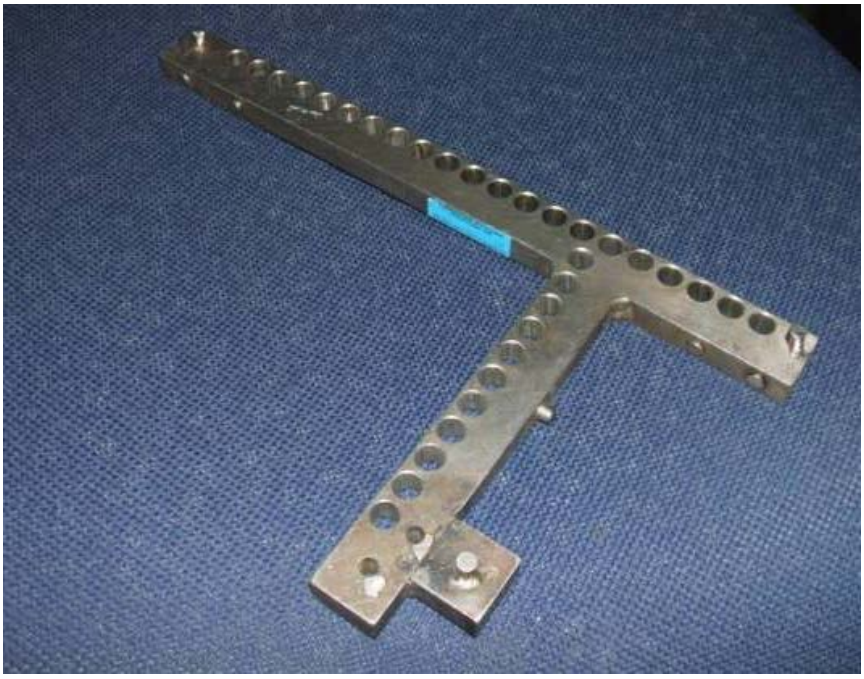

Figure 6. Bottom Side of the Template Used in Manual RSA Measurements
A dial indicator gauge was placed in predetermined numbered holes located around the template to obtain a profile of the abrasion depth. The "L" template was then turned 90 degrees to measure the other two sides of the rail seat area.)

The test plan was to measure RSA depth during the time rail seats were exposed when rail changes or rail seat repairs were conducted. The normal procedure followed by railroads includes the following major steps. Minor differences or additional steps are often followed but do not change the overall concept and time available to measure RSA:

1. Unclip fasteners from both sides of the rail being lifted
2. Lift and slide rail to one side or the other (Figure 7)
3. Follow with a crew removing existing rail pads, then clean rail seats (Figure 8)
    a. NOTE: At this point, rail seats are exposed and could be measured for RSA depth and photographed (Figures 9, 10)
4. Apply repair epoxy when RSA is of sufficient depth
5. Install new rail seat pads
6. Reinstall rail (or if a rail change, install new rail)
7. Adjust rail for proper longitudinal stress and reclip

The overall process from rail removal to reinstallation for a curve took several hours, but the "moving window" between steps 3 and 4 provided only a very short time, generally less than 5 minutes, to measure rail seats. Because of safety issues (rail movement, passing trains on adjacent tracks, and nearby equipment), the window for measurements was usually less than 5 minutes. A typical measurement of gauge and field side RSA depth and subsequent recording of the data required 45–50 seconds per tie; thus, collecting data at every tie to obtain a continuous tie-by-tie pattern of RSA through a full curve was not feasible.

Figure 7. Typical Maintenance Gang Conducting a Rail Change and RSA Repair
(Existing, old rail is being removed and set to the field (outside, right) side of track.
Note new rail has already been placed in the center of the track.)

Figure 8. Following the Rail Removal (Figure 7), Old Pads Are Removed and the Rail Seat Is Scraped Clean

(Note new pads, insulators, and clips have been distributed. At this stage, RSA *cannot* be measured due to logistics and work space conflicts.)

Figure 9. After Old Pads Have Been Removed, the Rail Seats Are Exposed

(The manual RSA measuring template and dial indicator are placed in position, and dial indicator readings are collected. In this photo the field (outside) of the rail seat is being measured.)

Figure 10. View from Figure 9 Looking Back to the Machine Repairing Rail Seats and Placing Pads in Position

(At this location, two RSA measurement groups are monitoring rail seat conditions, working in tandem. The "working window" for measuring RSA is from this site to about 30 feet (ft) toward the machine in this photo. Because the new rail in the center of the track is being placed into the rail seats directly behind the machine in the background, it is not safe to work more than 30 ft from this location.)

To speed up the RSA measurements as much as possible, TTCI fabricated two additional manual gauges. This allowed two teams of two people each (one measuring, the other recording data) to measure three to four ties in a row and then "leap frog" ahead of the other team, as Figure 10 shows. In one instance, sufficient personnel were available to use all three manual gauges, plus one person to document visual conditions (photograph) of each measured rail seat. Whenever the tie pad replacement and rail seat repair crew caught up, the measurement teams skipped ahead 10–15 ties and resumed measuring a batch of ties. Generally, the person photographing rail seats was positioned ahead of the measurement crews and would specify groups of ties to measure when RSA issues were noted.

This measurement procedure was cumbersome, but it allowed the overall trends and patterns of RSA on each selected curve to be documented and measured. However, the wide spacing between measurements is likely to limit the ability to link or correlate RSA to short wavelength track geometry features. Because it was not possible to measure every tie, it is not possible to determine from the data whether a single measurement is a short wavelength peak, with either more or less RSA at intermediate locations, or whether RSA varies proportionately between measurement locations. However, the RSA illustrated in Figure 4 suggests that RSA can vary considerably from tie to tie and therefore can occur on a fairly short wavelength.

For example, at the CSX St. Albans measurement site at MP 16, 30 measurements were made at relatively even spacing over a length of 282 ties for approximately 562 ft or approximately 19 ft per measurement. This means that the shortest wavelength detectable in the RSA measurements at that site is more than 40 ft, and accurate identification of the amplitudes is difficult for

wavelengths less than 80 or 100 ft. This implies that short wavelength phenomena such as typical down-and-out perturbations may not be detectable in any of the measured RSA data. The situation on the BNSF Needles and Alliance sites where measurements were made in clusters is more complicated, because measurements were made on three or four adjacent ties, but the clusters were much more widely spaced, leading to the possibility of missing considerable short wavelength information between the clusters.

To definitively identify short wavelength RSA, more frequent measurements over a longer distance are required. A faster, automated measurement system would have permitted more frequent measurements and would have been highly desirable; however, budget and time limitations prevented development and deployment of an alternative. The current project called for measuring RSA at only three railroad sites, with four to six curves selected at each site. With the cost to develop an automated system for this purpose deemed too high, to be cost-effective over manual methods, an automated measurement system would need to measure a rail seat every 10–15 seconds (or less). Should a future program in RSA evaluation need to collect data over many thousand ties, an automated (and fast) measurement device should be developed.

2.2 Track Geometry Measurements

For each measurement site, track geometry measurements were obtained from either the host railroad or FRA for the sections of track that were inspected. This data was used for the following two purposes:

1. Compare with RSA data to determine whether RSA could be correlated to specific features in the track geometry such as down-and-out lateral alignment and cross-level perturbations
2. Input to the NUCARS simulations

For the purposes of this project, it was requested that the data be provided in “space curve” format, the ideal format for input to NUCARS. Space curve data is preferred, because normal midchord offset measurements can miss critical information that it is not possible to reconstruct from the data [4]. It was requested that at a minimum the following data be provided:

- Curvature
- Superelevation/Cross level
- Gauge
- Alignment (either track centerline or left and right rail alignment)
- Vertical profile (either track centerline or left and right rail vertical profiles)

BNSF provided space curve data in the requested format from the Needles site, and FRA provided the data for the Alliance site on BNSF by using the DOT 218 measurement car. However, CSX was not able to provide space curve data from the St. Albans site.

The data available from CSX had been measured by using a form of midchord offset measurement. The midchord offset measurements for the profile and alignment data had an unusual measurement wavelength and was unsuitable for input to NUCARS. Therefore, for comparison to the RSA measurements on CSX and for input to NUCARS, the profile and alignment for CSX were reconstructed from the curvature, gauge, and superelevation data.

However, because of the measurement wavelengths for the available data information, it is very likely that some short wavelength variations in the vertical profile and alignment were not included in the simulations, although the gauge and cross level were correctly represented in the simulations. The missing geometry data may have resulted in lower wheel forces from the simulations.

2.3 NUCARS Simulations

A limited number of NUCARS simulations were conducted to estimate the vehicle dynamic response and wheel/rail forces that would be generated by typical freight cars running over the inspection sites. The results of the NUCARS modeling were then compared with the measurements of RSA from the sites and the measured track geometry from the sites to determine whether any correlations could be made between local track geometry features (such as down and out track perturbations), vehicle dynamic response, and RSA.

2.3.1 NUCARS Vehicle Model

The test different sites all have traffic from a mix of different rail vehicles. For example, the St. Albans site has primarily coal gondolas and hopper cars, whereas the Needles site has primarily intermodal freight cars. However, at all sites it is expected that the cars that generate the largest forces will be loaded to a maximum axle load of 36 tons and use some form of three-piece freight car trucks. Therefore, for the limited number of simulations conducted for this segment of the project, only one vehicle was simulated: a loaded, 286,000-pound (lb), four-axle coal gondola with standard three-piece freight car trucks with variable friction damping and constant contact side bearings. The basic dimensional information for this car was as follows:

Truck spacing: 486 inches (in) (40.5 ft)

Axle spacing in truck: 70 in

Total weight: 286,000 lb

Carbody weight: 266,500 lb

Carbody center of gravity height above rails: 83 in

In a future segment of this project, it is recommended that the operation of a few other vehicles, such as loaded intermodal cars, be simulated to determine whether other car types generate similar responses and effects on RSA development.

Wheel profiles were measured on four typical coal hoppers that ran over the St. Albans site. Figure 11 shows the results of NUCARS trial simulations conducted with some of these different profiles. It can be seen that different wheel profiles can generate different levels of wheel/rail forces, although the trends of higher L/V ratios in the body of the curve are the same. From these trial simulations, the wheel profile that generated the largest truck side L/V ratios was selected for use in all further simulations. The truck side L/V ratio was selected as the primary performance parameter, because it represents the combined effect of two adjacent axles acting on the rails.

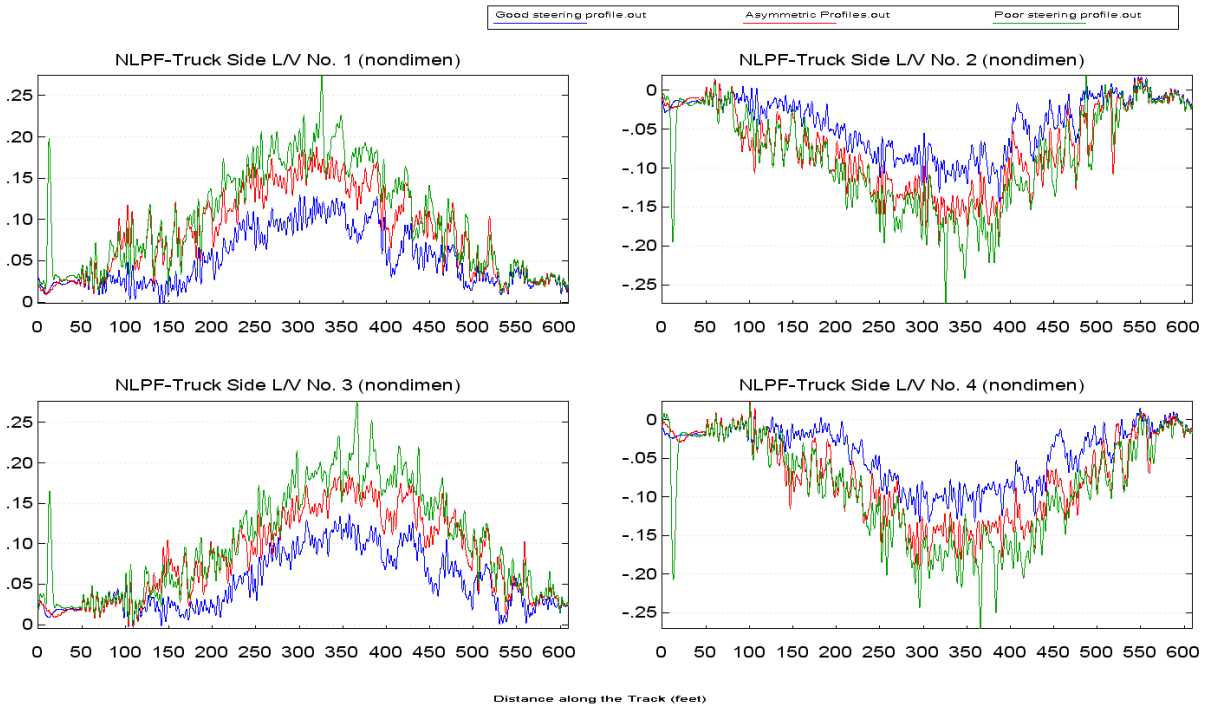

Figure 11. Example Comparison of Truck Side L/V Ratios from NUCARS Simulations Using Different Combinations of Wheel Profile Measurements

(The blue line uses a single wheel profile with good steering characteristics; the red line uses a pair of asymmetric wheel profiles as measured on one axle; the green line uses a single wheel profile with poor steering characteristics.)

2.3.2 NUCARS Track Model

To accurately simulate the dynamic response of the rails on the ties and the consequent forces and moments in the rail seats, the track model capability in NUCARS was used to simulate the rails, fastening system, ties, and ballast. Figure 12 illustrates an example of a two-layer track model, similar to what was implemented for this project. Details of the track model were adjusted to meet the requirements of this project.

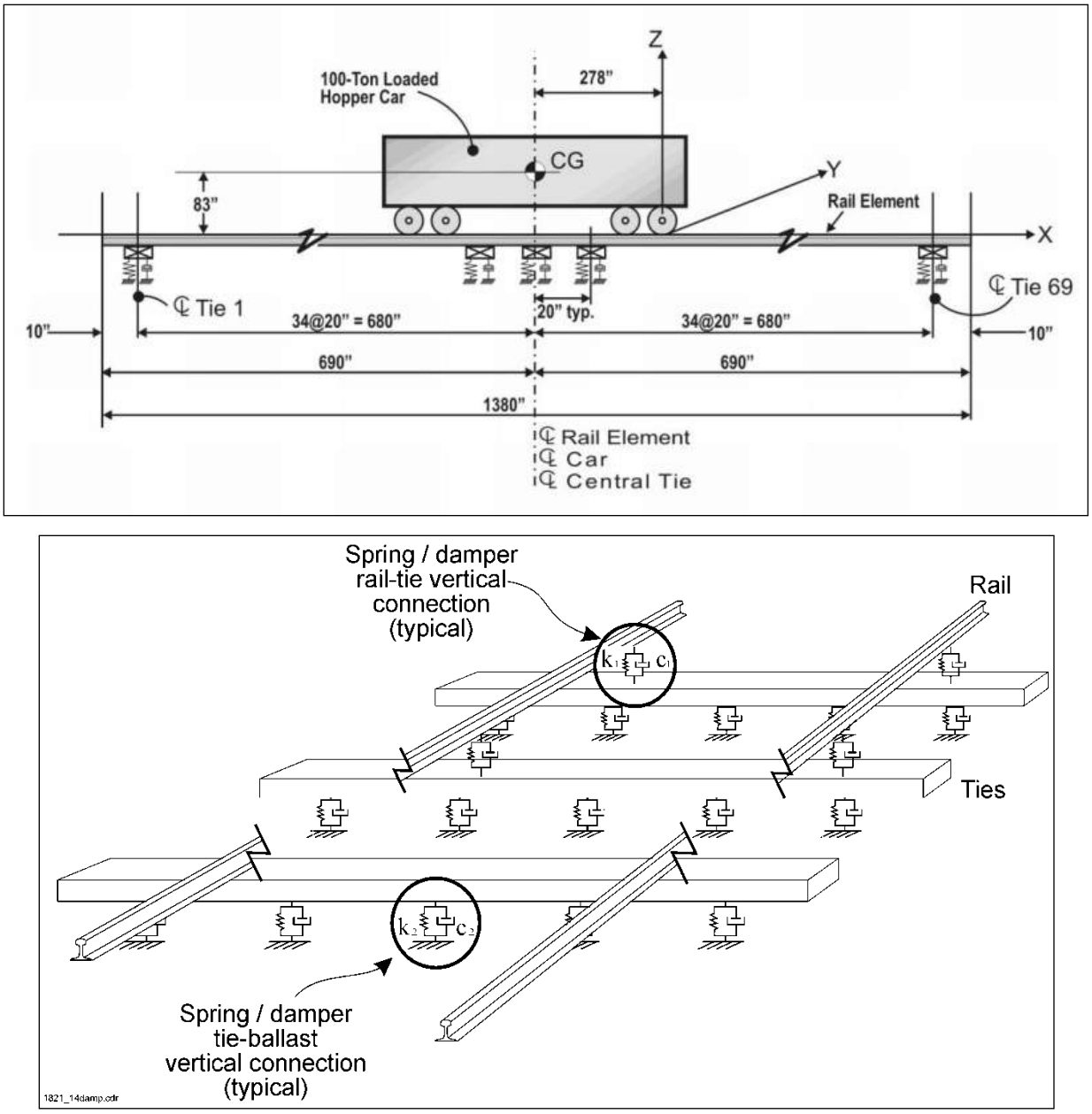

Figure 12. Example of Two-Layer Track Model in NUCARS

The NUCARS track model used for this project included the following basic assumptions:

- Flexible rails, with motions in the vertical (*z*), lateral (*y*), and roll (around *x*) directions, including vertical, lateral, and twist bending modes. Sufficient flexible modes were provided to include the pinned-pinned mode for each flexible direction, based on the tie spacing.
- Flexible ties, with vertical (*z*), lateral (*y*), and roll (around *x*) motions, including the first seven modes of vertical bending. Ties were spaced 24 in apart.

- Rail seats and fasteners were represented by two vertical and two lateral connections per rail seat, one on each side of the base of the rail.
- Ballast was represented as eight discrete vertical and lateral connections between each tie and the ground.

Because detailed measurements of fastener and pad characteristics and local ballast stiffnesses were not available, representative values for these parameters were selected on the basis of experience with previous measurements and model simulations of similar track. For this phase of work, the NUCARS simulations assumed ballast and track fastener conditions (stiffness, preload, etc.) to be identical at each tie. The track parameters were assumed to be the same for all the sites modeled. NUCARS permits input of different conditions for the ballast at each tie and different conditions for each fastener. For future phases of work, these parameters could be varied from tie to tie and site to site, as required or appropriate.

Rail profile measurements from each measurement simulated were used as inputs to the model.

The NUCARS track model uses the wheel and rail profile measurements to calculate the wheel/rail contact geometry for each wheel at each simulation integration step as the vehicle moves along the track. The wheel/rail contact geometry calculations include the effects of the rail vertical, lateral, and roll motions at each wheel. The penetration contact model used in the NUCARS track model permits calculation of up to 10 overlapping contact points per wheel.

NUCARS permits outputting the forces in the rail seats and fasteners at any selected tie. As noted above, two vertical and lateral connections were used per rail seat. These connection forces were converted to a single rail seat vertical force and rail seat roll moment to allow comparisons between ties and sites.

3. Survey Measurements and NUCARS Simulation Results

TTCI developed detailed test plans for field inspection and measurements. These were reviewed by the FRA COTR and Volpe engineering staff to ensure data obtained satisfactorily addressed future requirements of the planned modeling effort.

Data collected included:

- Recent track geometry measurement outputs
- Field inspection photos and notes on RSA variation at the site
- Measurements of RSA depth, pattern, and appearance, at locations noted by the photographer as having more severe RSA
- MiniProf rail profiles collected at various locations around a curve
- Train operation characteristics—load, line density, traffic volume, speeds, direction, braking, etc.

Three survey sites were identified, one on CSX and two on the BNSF. Once the data at the CSX site was collected, the methods used to correlate track location with track geometry information and NUCARS simulation results went though several iterations to select a wheel profile for use in the simulations and to develop methods for displaying and comparing the NUCARS simulations with the track data. In addition, improved field measurement techniques and additional RSA templates were fabricated to further streamline future RSA depth collection efforts. These efforts required several months to complete, delaying the time frame when the BNSF sites could be inspected until early 2011.

Survey measurements and corresponding NUCARS simulation results are presented for each of the three sites in the following three subsections.

3.1 Site 1 – CSX Coal River Subdivision near St. Albans, WV

The first location for measuring RSA on this project was offered by CSX on its Coal River Subdivision near St. Albans, WV. This is a single track line with virtually 100-percent coal traffic, with loaded unit trains traveling in one direction and empty returns in the opposite direction. A nearby large town, Charleston, WV, has an average of 43 in of precipitation per year, making it the wettest site surveyed.

In early July 2010, six curves were selected for measurement on the basis of length, accessibility, and visual indications, suggesting RSA was present. Track maintenance schedules and measurement resources allowed these curves to be inspected in detail and RSA measured during track work performed in August 2010. Table 1 lists the details of the actual measurement sites at St. Albans.

Table 1. Description of Measurement Sites at St. Albans, WV

Milepost (MP)	Curvature (deg)	Super-elevation (inch)	Balance Speed (mph)	Normal Operating Speed (mph)	Rail Measured (High/Low)	Comments, Notes, etc.
26.3	11	2.0	16		Low	
22	2	1.0	27	25	Low	Compound curve
20	15	1.0	10	25	High	Curvature ranges from 14 to 16 degrees Superelevation ranges from 0 to 1 in
19	12	3.0	20		High	Wayside lubricators nearby, supplemented by Hy-Rail application
17	5	0.5	12	15–20	Low	Wayside lubricators nearby, supplemented by Hy-Rail application
16	8	2.0	20		Low	Wayside lubricators nearby, supplemented by Hy-Rail application

Figure 13 through Figure 15 show the abrasion data collected in the curves at MP 16, MP 17, and MP 19, respectively. These curves were measured with the more accurate manual gauge. The other three curves were measured with the automated system only. The first 208 ties of the curve at MP 19 were measured with the automatic machine until rain damaged the equipment. A large amount of scatter in that part of the plot is apparent (Figure 15). A similar amount of scatter was seen in the other three curves. Because of this, results from those curves are not shown. In Figure 13 through Figure 15, the *Average* is the aggregated value of the RSA depth measurements taken on the rail seat. Positive values indicate wear into the tie. The *Difference* is the average of the data from the field side of the rail seat minus the average of data from the gauge side of the rail seat. The abrasion measurements are referenced to the original cant of the rail seat. Therefore, a difference value of zero indicates no rail roll, but the rail will be canted to the angle that was built into the rail seat. A positive difference indicates abrasions that would tend to cause the rail to roll (cant) outward relative to the original rail seat and a negative difference would cause the rail to roll (cant) inward.

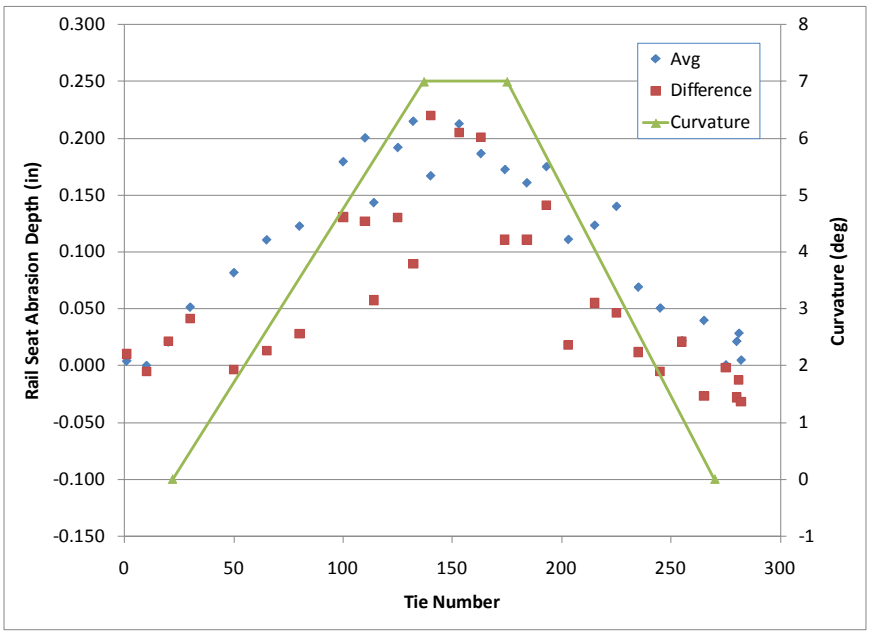

Figure 13. Low Rail MP 16.78–16.68; This Curve Shows a Very Clear Relationship between Track Curvature and RSA Depth

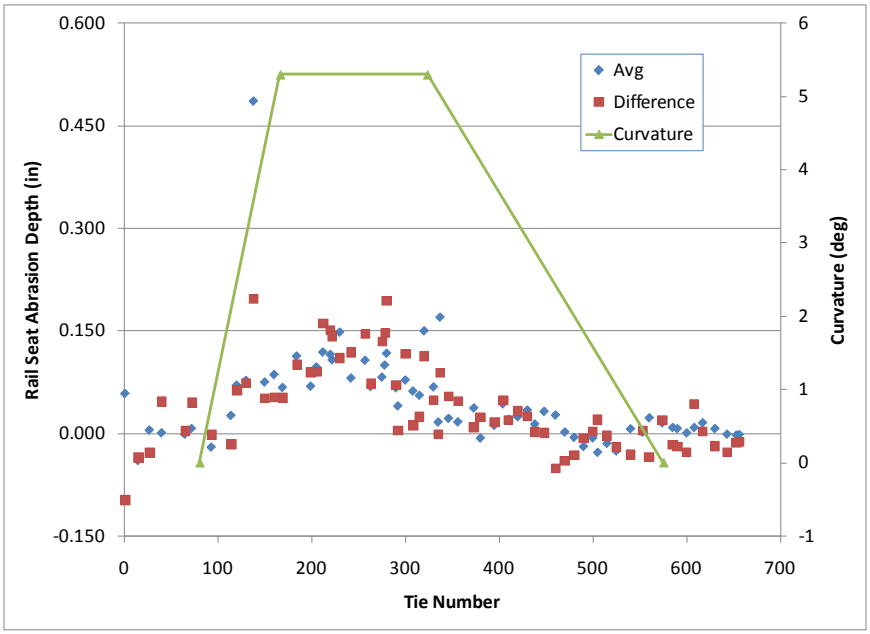

Figure 14. High Rail MP 17.49–17.3, although Less Distinct Than the Curve at MP 16; This Curve Shows a Correlation between Curvature and RSA Depth

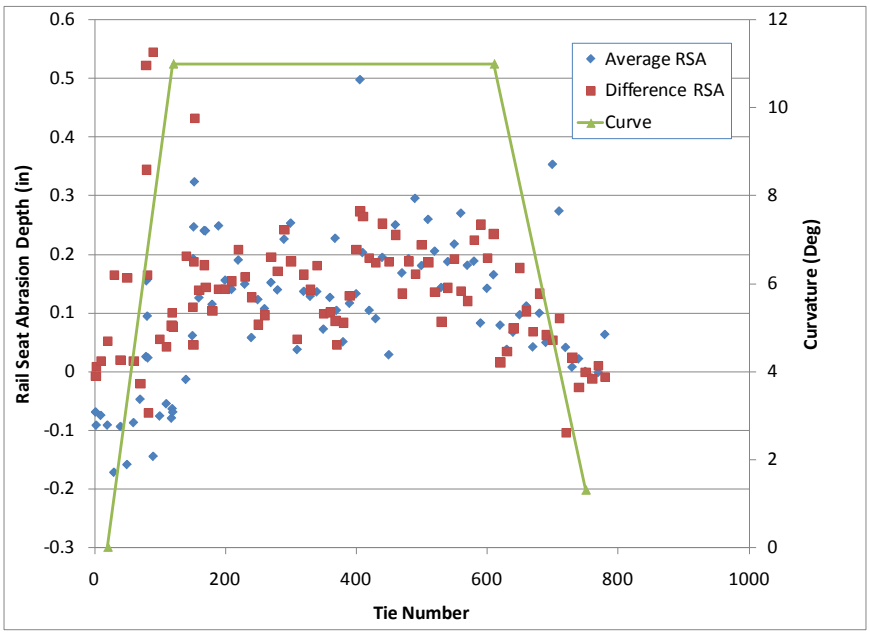

Figure 15. High Rail MP 19.7

(The first 208 ties in the spiral and beginning of curve were measured with the laser trace machine before wet weather damaged it, and the rest of the ties were measured with the manual gauge. The larger scatter apparent in the laser trace machine data is thought to be to the result of the large machine tipping on its relatively small triangular base.)

On this line segment, track maintenance work was limited on these curves to one rail per curve, either the high or low rail, as shown above.

Results from inspecting RSA on the Coal River Subdivision suggest the following:

- Significant RSA depth at some locations but not a uniform depth on any curve
  - RSA varied significantly from location to location around each curve.
  - All ties had been previously repaired, some possibly twice.
  - The prior repairs impacted the ability to accurately measure RSA, and it was impossible to differentiate current wear from older wear.
  - RSA depth often increased within the limits and directly adjacent to dirt road crossings where moisture was trapped as the result of limited drainage.
- Data collected of RSA average depth and difference (cant) suggests
  - As RSA depth increases, so does rail cant
  - At the curves, all cant resulting from RSA was outward (more RSA depth on field side than gauge side)
  - A close correlation with position in curve and RSA depth
    - More curvature results in more RSA depth and cant
      - Typically, at the tangents there was little or no measured RSA
      - RSA depth gradually increased through the spiral

- RSA depth remained generally uniform through the body of the curve (not including the spiral)
- A few isolated locations of deeper RSA did not correlate with variations in measured track geometry or predicted wheel/rail forces. These locations tended to be near grade crossings or areas where previous rail seat repairs had failed maintaining track structure. It is suspected that the RSA near grade crossings is the result of poorer drainage and higher levels of moisture under the rail seats at these locations
- The scatter and large RSA values in the first 208 measurements at MP 19.7 shown in Figure 15 are probably suspect because of problems encountered with the laser measurement device

Two curves were analyzed and summarized in data plots generated to show RSA depth and difference (cant angle) versus distance along the curve. RSA depth is based on the average of all readings (both field and gauge side) for each rail seat. RSA difference subtracts the average gauge side RSA depth from the average field side RSA depth. Thus, a positive difference value indicates outward cant of the rail or deeper RSA on the gauge side compared with the field side. A difference of 0.1 in corresponds to approximately 0.95 degrees of rail cant.

Figure 16 compares measured RSA depth, RSA difference (RSA cant), to track geometry and NUCARS predictions of wheel/rail forces for MP 16, with direction of travel from right to left in the graph.

The first graph in Figure 16 shows the measured track curvature and superelevation/cross level. The second graph shows the manual measurements of average RSA depth and RSA depth difference (field-gauge) for the right/low rail. The third graph shows the measured track gauge and alignment as well as the left/high and right/low rail cants as measured by the track geometry car.

The track geometry data (curvature, superelevation, alignment, and gauge) was used as input to the NUCARS simulations. The fourth and fifth graphs show the NUCARS predictions of lead axle single wheel L/V ratios and lead truck side L/V ratios, which were performed with the assumption of dry rail (rail friction coefficient of $\mu = 0.4$). In this graph, a positive L/V ratio on the right rail and a negative L/V ratio on the left rail represent gauge-spreading forces. Note that in actual practice the friction coefficients in this curve are probably different as a result of the presence of track lubricators in the vicinity, which would result in somewhat different forces and dynamic response. However, friction levels were not measured.

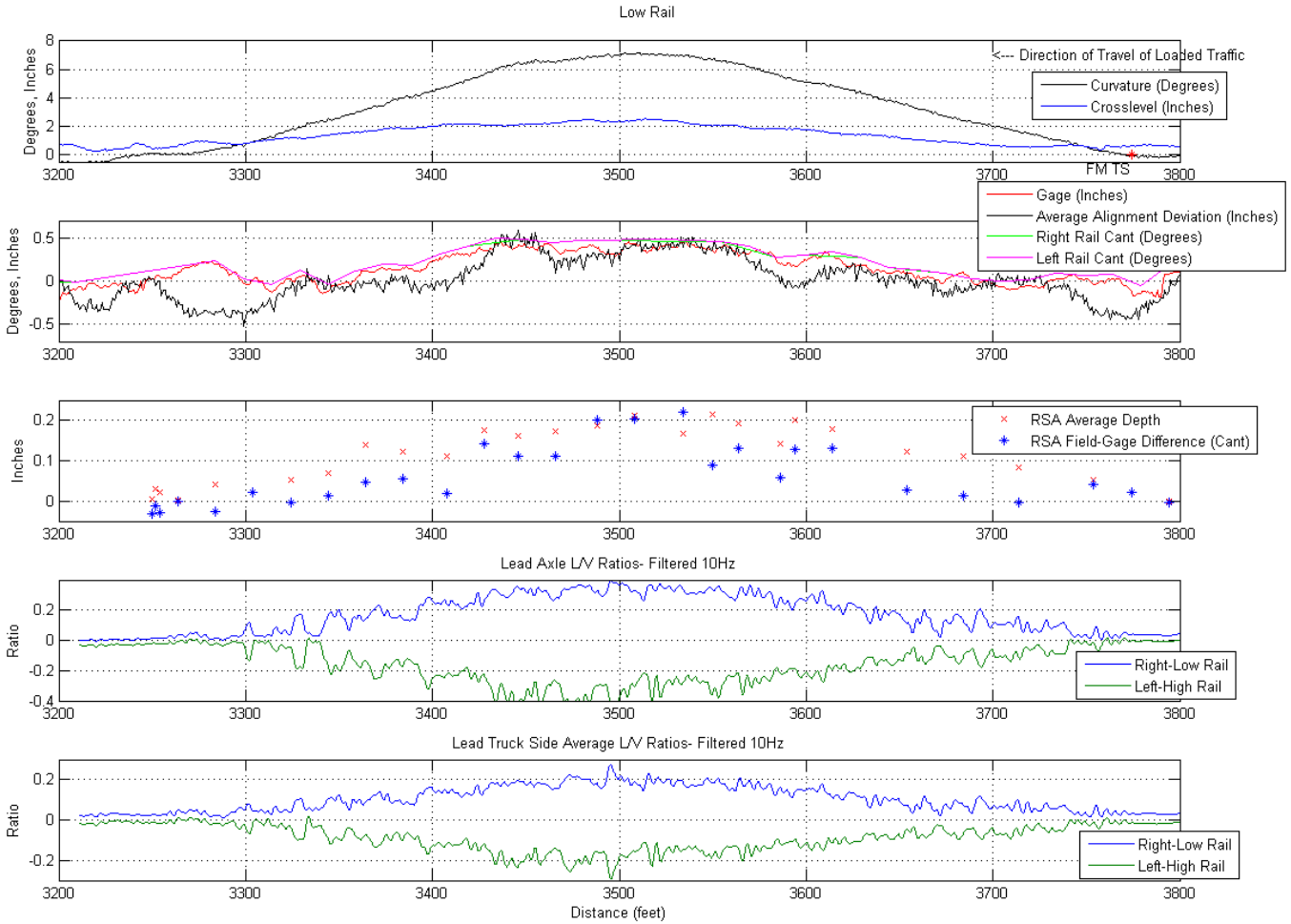

Figure 16. Curve Data for MP 16; Distance along Curve Measurements and Predicted Car Performance of a Loaded Hopper
(Top to bottom shows curvature and superelevation, measured RSA average depth and difference, track geometry data, predicted lead axle L/V, and predicted lead truck side L/V.)

Figure 17 shows the corresponding NUCARS predictions of rail seat vertical forces and roll moments. This graph shows the forces acting on the tie that is located near distance 3,596 ft in Figure 16. This is in the entry spiral nearest to the spiral to curve location at the beginning of the curve. At the left side of the plot, the vehicle has not yet arrived at the tie. Then, each axle approaches and travels over the tie, and the corresponding rail seat forces and moments are shown. Axle 1 arrives first, shown on the left side of the graph, and Axle 4 is last shown on the right side.

Figure 18 shows the NUCARS predictions of rail seat vertical forces and roll moments for the tie that is located nearest to distance 3,478 ft in Figure 16. This is at the start of the exit spiral (curve to spiral location) at the end of the curve.

In these two graphs, negative vertical forces indicate pressure downward on the rail seat, and positive roll moments indicate moments that would cause the rail to roll outward and apply greater pressure to the outside of the rail seat.

The rail seat moment can be seen to vary considerably with location in the curve. At the entry spiral (3,596 ft), the roll moments on the high (left) rail seat only reach 15,000 in-lb and undergo a reversal when the second axle of the truck passes over. On the low (right) rail, the moments are much higher and do not reverse. At the end of the curve near the exit spiral (3,478 ft), the moments on both rails are much higher, and they do not reverse on either rail, indicating that both rails have a tendency to roll outward, which is consistent with both the RSA measurements and rail cant measurement at this location.

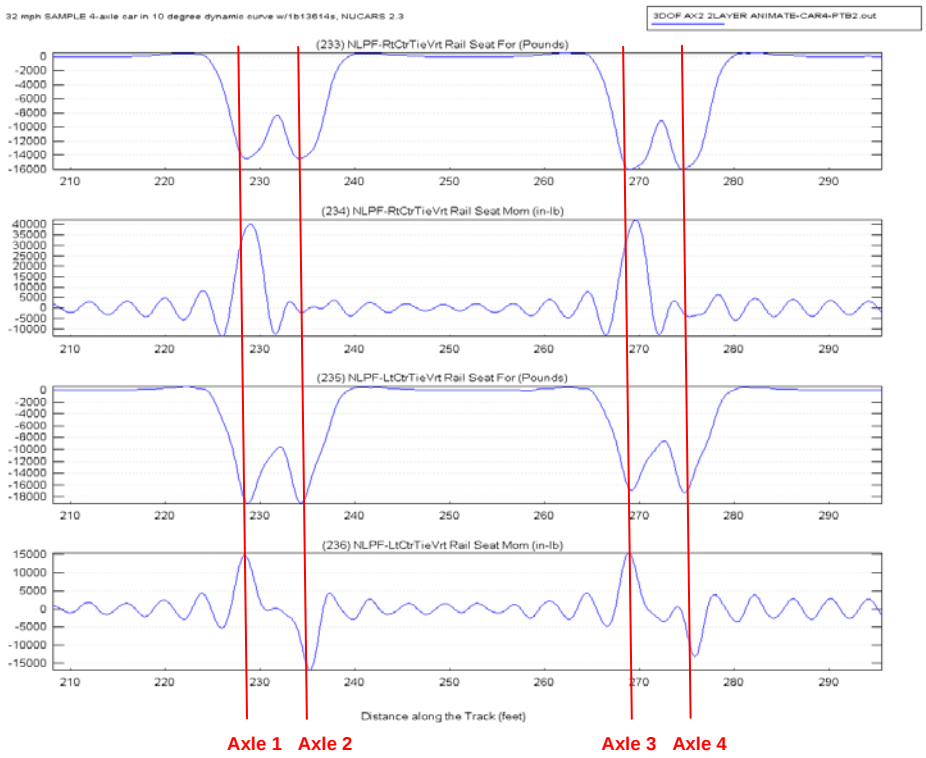

Figure 17. Rail Seat Vertical Forces and Roll Moments for MP 16 at Tie Located at 3,596 ft

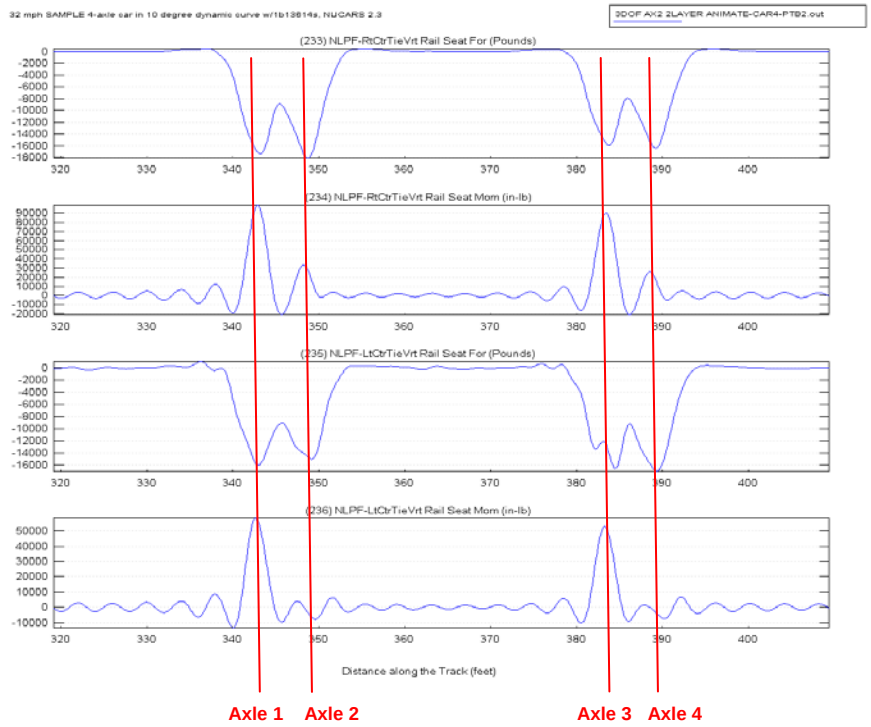

Figure 18. Rail Seat Vertical Forces and Roll Moments for MP 16 at Tie Located at 3,478 ft

The results show that although the curve is relatively sharp, the L/V ratios are not excessive, but they are applying gauge-spreading forces to the rails. The differences in roll moments as the leading and trailing axles of each truck pass over the tie are because the lead and trail axles contact the rails in different positions, with the leading axle in hard flange contact on the high rail generating higher L/V ratios on the right low rail (Figure 19) than the trailing axle (Figure 20), as would normally be expected for operation on dry rails. The lateral positions of the contact affect how the lateral and vertical forces generate the roll moments seen at the rail base. However, the largest roll moments are consistent with rolling both of the rails outward, as was seen for the low rail RSA measurements.

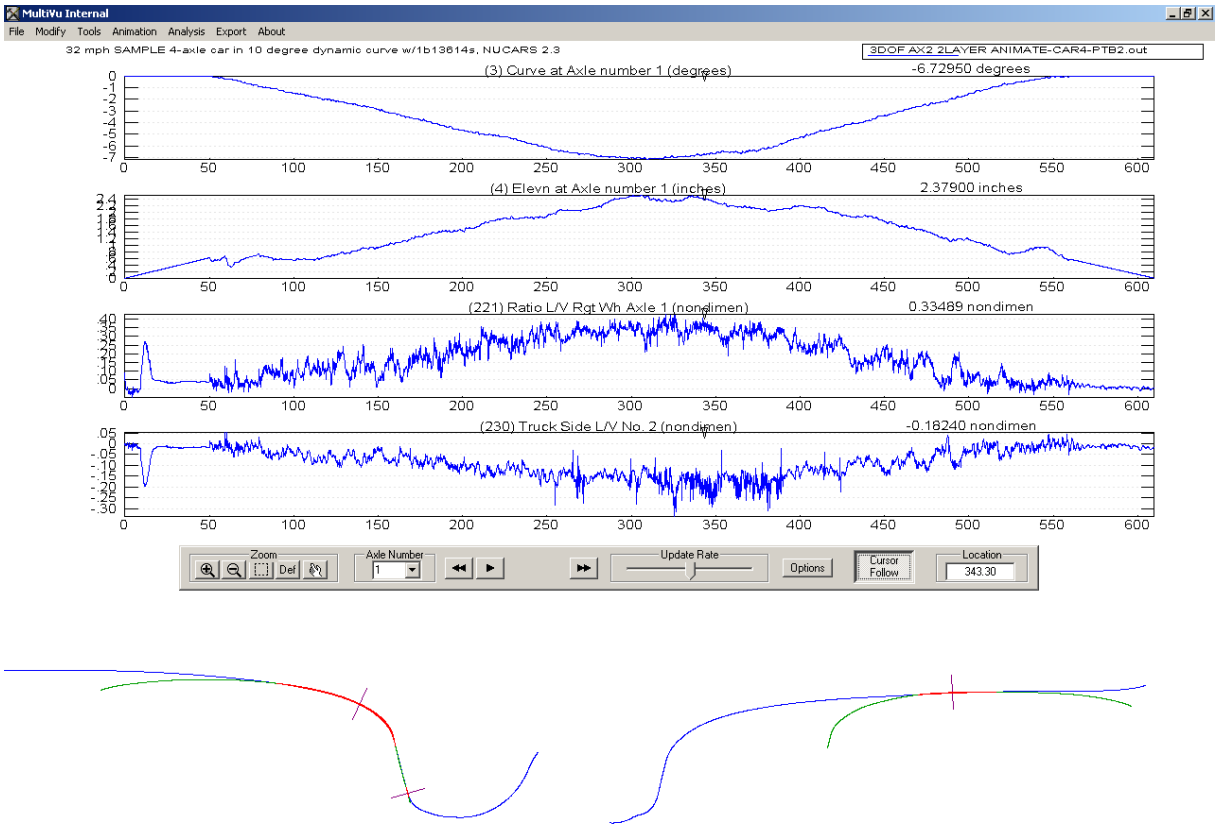

Figure 19. Wheel/Rail Contact Geometry for Axle 1 at 3,478 ft along the Track for MP 16 with Corresponding Left and Right Wheel L/V Ratios, Showing Hard Flange Contact on High Rail

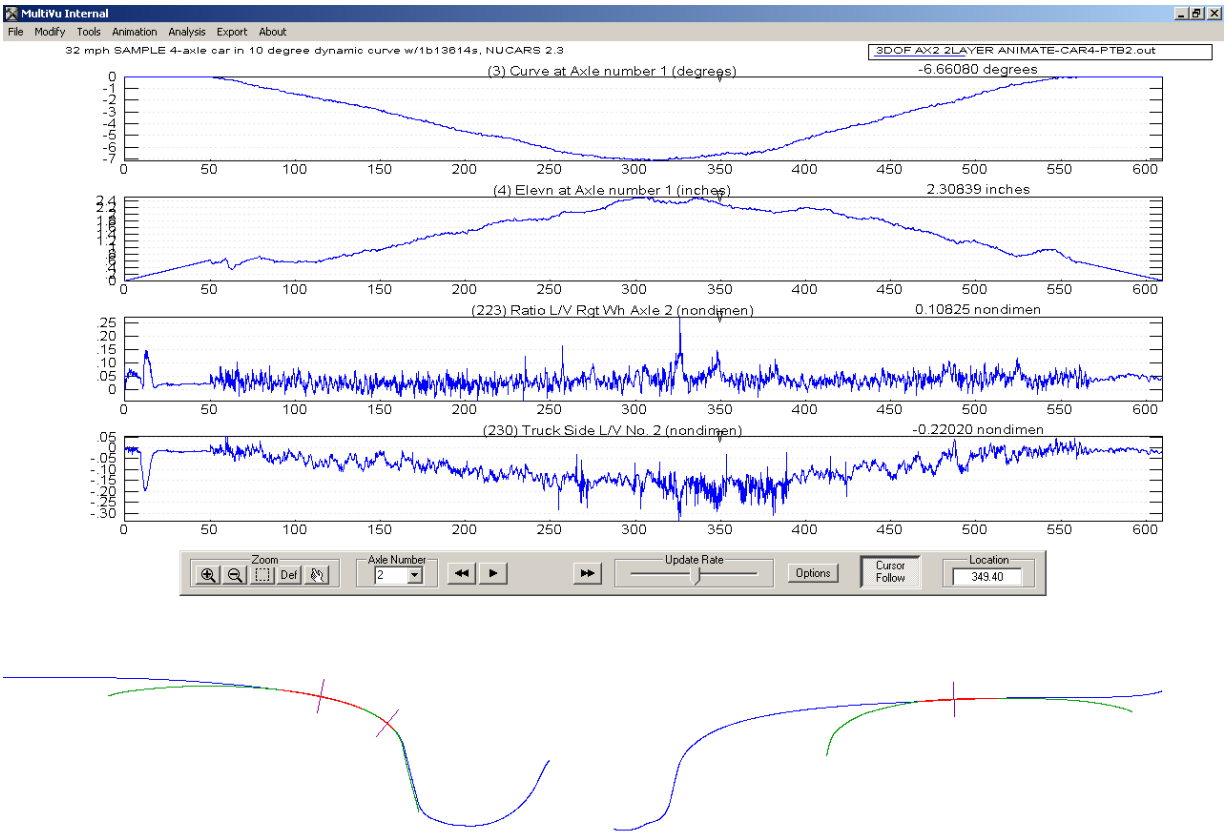

Figure 20. Wheel/Rail Contact Geometry for Axle 2 at 3,478 ft along the Track for MP 16 with Corresponding Left and Right Wheel L/V Ratios, with High Rail Wheel Contacting in the Flange Root

Figure 21 shows the relationship of measured RSA, RSA field-gauge (RSA Cant) for MP 17, with direction of travel from right to left in the graph. RSA measurements are compared with the NUCARS predictions, which were performed with the assumption of dry rail (rail friction coefficient of $\mu = 0.4$). In this graph, a positive L/V on the right rail and a negative L/V on the left rail represent gauge-spreading forces. Note that in actual practice, the friction coefficients in this curve are probably different because of the presence of track lubricators in the vicinity, which would result in somewhat different forces and dynamic response. However, friction levels were not measured.

Figure 22 shows the corresponding NUCARS predictions of rail seat vertical forces and roll moments, with Axle 1 on the left side of the graph and Axle 4 on the right. These forces are at the tie that is located near to distance 2,154 ft in Figure 21. L/V ratios, rail seat forces, and moments for MP 17 are slightly less than for MP 16, because the curve is less sharp. However, the trends are very similar.

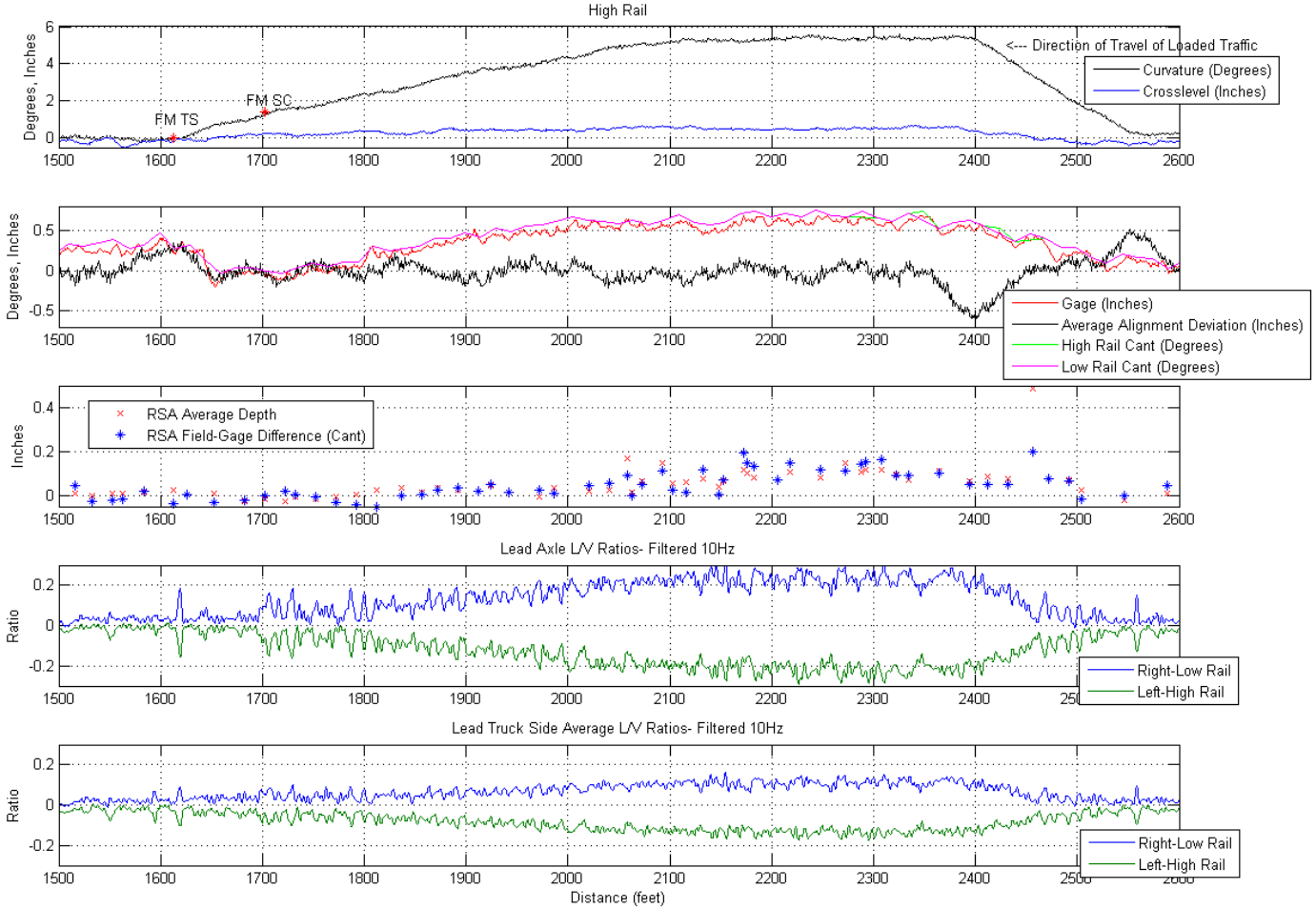

Figure 21. Curve Data for MP 17; Distance along Curve Measurements and Predicted Car Performance of a Loaded Hopper
(Top to bottom shows curvature, RSA depth and cant, track geometry data, predicted lead axle L/V ratio, and predicted lead truck side L/V ratio.)

.

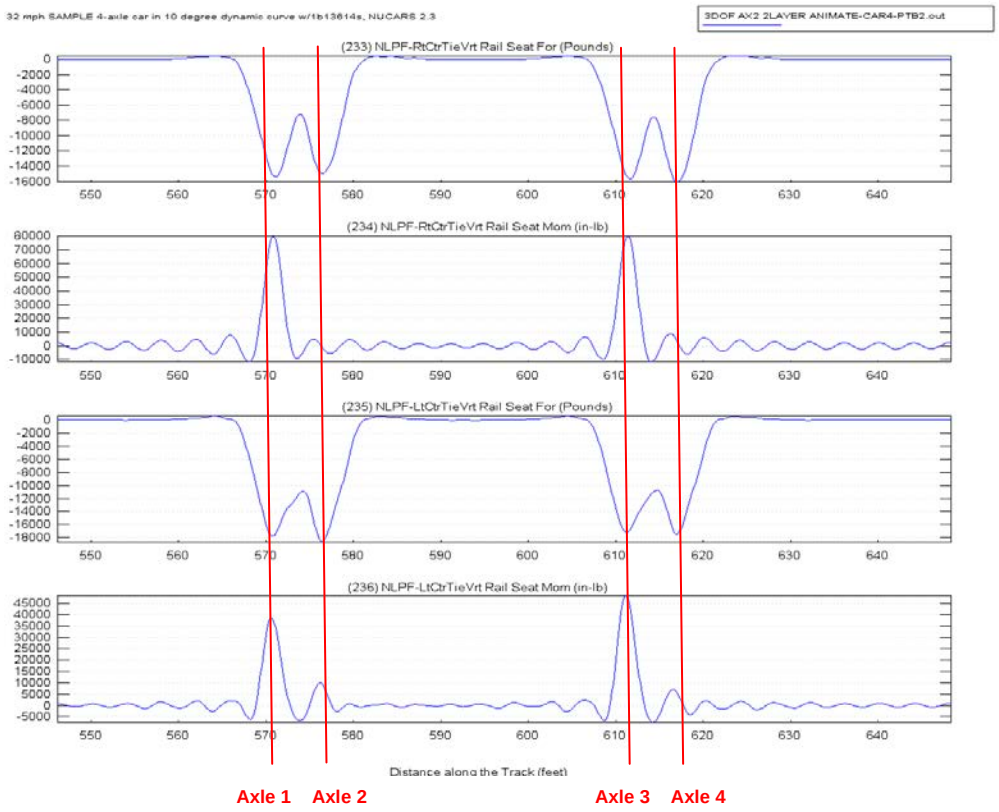

Figure 22. Rail Seat Vertical Forces and Roll Moments for MP 17 at Tie Located at 2,154 ft

Data in Figure 16 and Figure 21 shows the trend of RSA depth increasing from nearly zero in tangent track to some measurable value in the curve, transitioning from zero to approximately 0.2 in. in the spirals. RSA data in Figure 16 does not show any significant localized severity while that shown in Figure 21 indicates localized short segments of deeper RSA at approximately 2,180 ft and a deeper pocket at approximately 2,460 ft. Minor variations in lateral vehicle curving forces are predicted near the 2,460 ft location, along with localized alignment deviations near that site. However, the changes in vehicle performance are noted *after* the variations in RSA, suggesting that the vehicles were responding to minor variations in rail cant or alignment and not directly causing RSA.

Historical trends in track geometry measurement data would need to be evaluated to determine whether the alignment deviation has been in place for some time, and if so, is it the result of localized support conditions or the reaction to localized and long-term curving performance?

Figure 23 to Figure 25 show examples of rail seat conditions noted during the inspection.

Figure 23. Curve 17, Typical Rail Seat Conditions near Tie 205
(Ties measured with Tie 0 at the beginning of the curve in direction of loaded traffic, located at approximately 2,150 ft.)

Figure 24. Curve 17, View of Rail Seat Previously Repaired
(Epoxy used in former repair was still in place and could not be removed; thus, impaired ability to measure actual RSA depth. Ties measured with Tie 0 at the beginning of the curve in direction of loaded traffic, located at approximately 1,750 ft.)

Figure 25. Curve 16, Tie 104, Left Is Field Side, with More RSA Depth on the Field Side of the Rail Seat, and It Results in Outward Tilt (cant) of the Rail
(Ties measured with Tie 0 at beginning of curve in direction of loaded traffic, located at approximately 3,580 ft.)

Data was collected on the six curves listed above, and to date, comparisons of RSA with measured track geometry and with NUCARS simulations have been performed only for the curves at MP 16 and MP 17 shown above. A review of RSA measurements from curves at MP 16, MP 17, and MP 19 indicated that depth and rail roll (cant) follow curvature and superelevation with little or no deviations. The few isolated instances of deeper RSA did not correlate well with any localized track geometry anomalies or changes in predicted truck curving performance. Because of the problems with the automated measuring device, the RSA measurements from the other three curves were too scattered to make a clear evaluation.

3.2 Site 2 – BNSF near Needles, CA

The second location offered for RSA inspection was provided by BNSF near Needles, CA. Work crews were scheduled for early (first quarter) 2011; thus, preinspection of potential curves was conducted January 11–12, 2011, and rail replacement gangs were scheduled for the first week of February. The preinspection methods were identical to those followed on the CSX St. Albans site. Each potential curve on the work program was inspected and documented. To aid in correlating RSA measurements to track geometry data, the point of tangent to curve was located for each curve. Ties were then numbered, and every tenth tie was marked in the field in advance of track work. MiniProf rail profiles were also collected at all curve points and midcurve locations.

Because of changes in work schedules and priorities, some curves preinspected in January were not included in the final program, and other curves were substituted. Table 2 lists the details of the curves measured during the February 2011 work window at Needles.

Table 2. Description of Measurement Sites at Needles, CA

Milepost (MP)	Curvature (deg)	Super-elevation (inch)	Balance Speed (mph)	Normal Operating Speed (mph)	Rail Measured (High/Low)	Comments, Notes, Etc.
589	3.75	5	28		High	
588.5	2.5	2	34		Low	
588.2	3.75	2.5	31		Low	
584.5	3.25	4	44	15–20 uphill 25–55 downhill depending on train type	Low	Block signal, insulated joints in both rails near mid-curve Visual evidence of gauge face lubrication
583	3.75				Low	

The Needles site differs significantly from the St. Albans site. The concrete ties at the Needles site had never been repaired since first installed in early 2000. Traffic over the Needles curves is predominantly intermodal (mostly double-stack containers and piggyback traffic) with some mixed freight. No significant coal or unit trains operate over this line. This track segment is a double-track transcontinental main line, with frequent train passage. The line being worked for rail replacement was Main 1, which normally handles eastbound trains. Normal traffic patterns and operation over these curves show train speeds of 50–55 miles per hour (mph), running downgrade. Because these trains are approaching a mandatory crew change at Needles (MP 578), the curve closest to Needles (MP 583) may be subjected to slower or slowing trains, whereas all other curves measured normally have traffic at the full allowable track speed (50–55 mph).

Of possibly greater influence on curving forces, occasionally traffic congestion or track work on Main 2 requires westbound trains to be routed to Main 1. These trains depart the Needles crew change from a complete stop and immediately encounter a continuous ascending 1 percent grade, usually limiting westbound trains to 15 mph over all curves in the RSA measurement area. Exact traffic mix was not determined; however, local BNSF staff estimated 80 percent of the trains over the five curves measured for RSA operate at or near 50 mph, with remaining traffic in the 15-mile per hour range.

Another major difference is climate. The St. Albans site is in an eastern area subjected to winter snow and year-round rain. The Needles location generally has less than 10 in of precipitation per year and is considered a desert area.

Of all five curves inspected at the Needles site, none had significant RSA. The deepest continuous RSA was in the 0.05-inch range, compared with approximately 0.20 in observed at the St. Albans site. Overall observations of RSA conditions at the Needles site include:

- No deep RSA was noted at any location, deepest RSA recorded was approximately 0.05 in
- All pads, clips, and insulators were replaced as part of rail work
- Only the curve at MP 584.5 showed any significant RSA, and it was in the initiation stages
- The RSA at MP 584.5 indicated the RSA would tend to roll the inside rail inward

Figure 26 to Figure 30 show RSA results for the five curves at Needles. Imposed on each figure are the suggested curvature locations based on track chart information only. For Figure 26 to Figure 30, the numbers shown along the central axis represent tie numbers to allow correlation with RSA data and photos. Because tie spacing is 2.0 ft, the distance in feet is simply twice the tie number. To aid comparison with all curves inspected at Needles, the RSA depth/cant scale has been made the same to emphasize that there was little RSA depth measured at all curves, except at MP 584.5. Figure 31 shows typical RSA from the curve at MP 584.5.

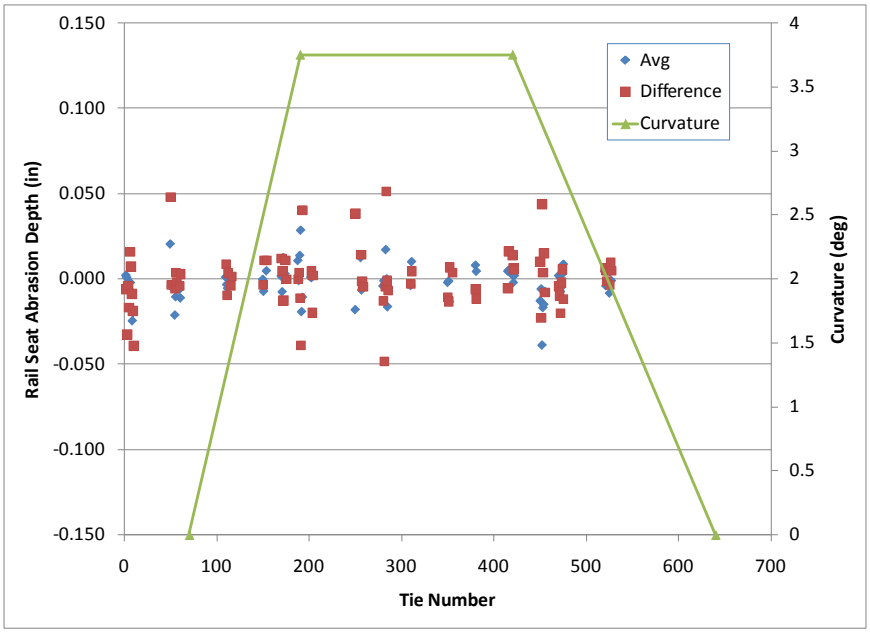

Figure 26. High Rail MP 589 Average RSA and RSA Difference(cant); Shows Almost no RSA Depth

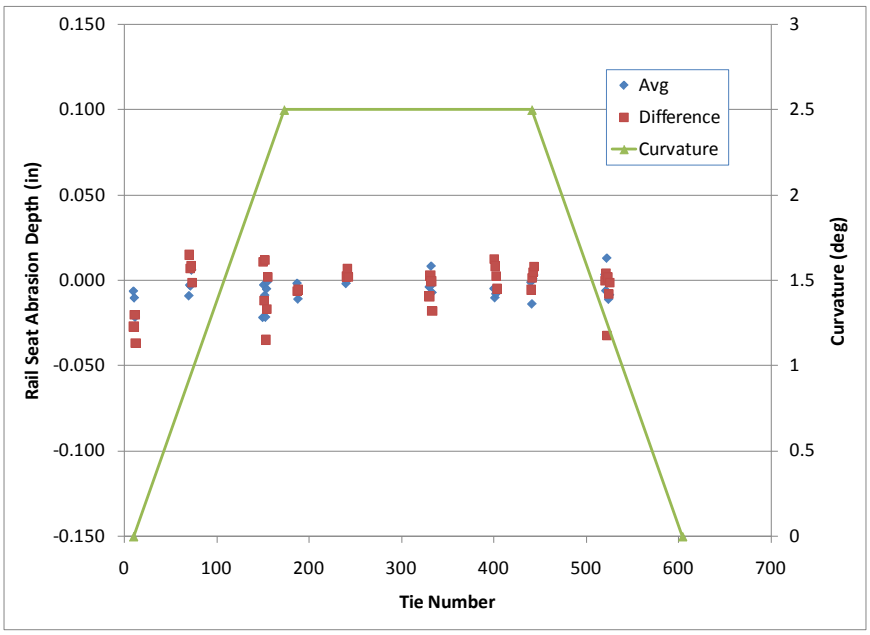

Figure 27. Low Rail MP 588.5 Average RSA and RSA Difference (cant); Shows Almost no RSA Depth

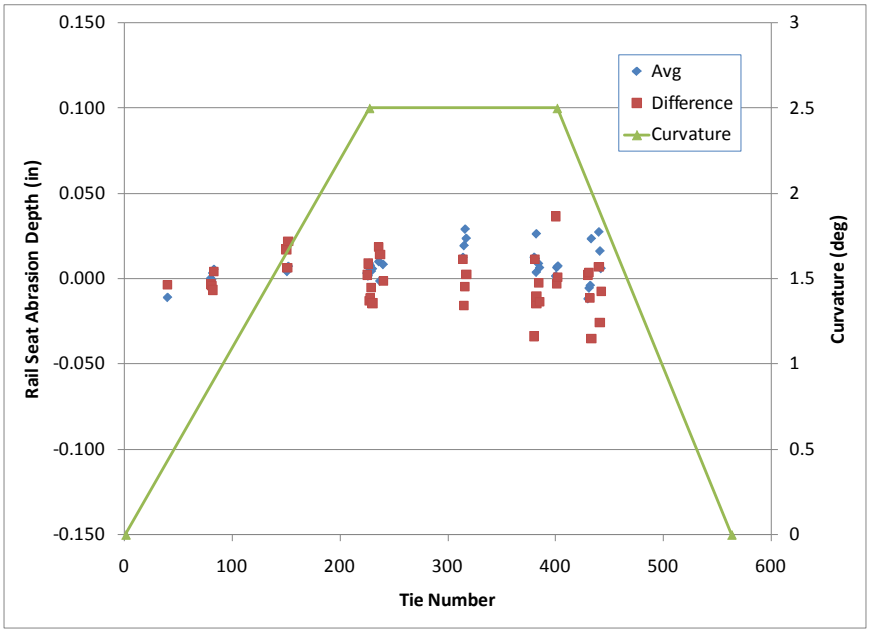

Figure 28. Low Rail MP 588.2 Average RSA and RSA Difference; Shows a Very Slight Tendency for Inward Cant (rail tilt) toward the End of Curve; Direction of Predominant Traffic Is Left to Right

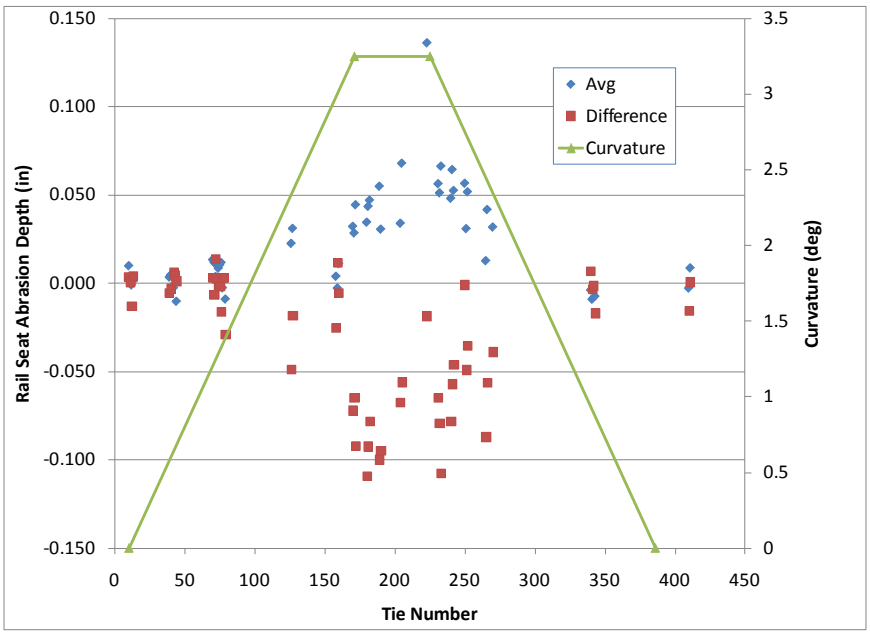

Figure 29. Low Rail MP 584.5 Average RSA and RSA Difference (cant); RSA Depth Is near Zero, Except in Full Body of Short Curve

(RSA difference is negative in the curve, indicating inward cant (tilt). Photos (Figure 31) confirm this inward tilt. Note that there is a block signal, with insulated joints, both rails near midcurve, near Tie 205.)

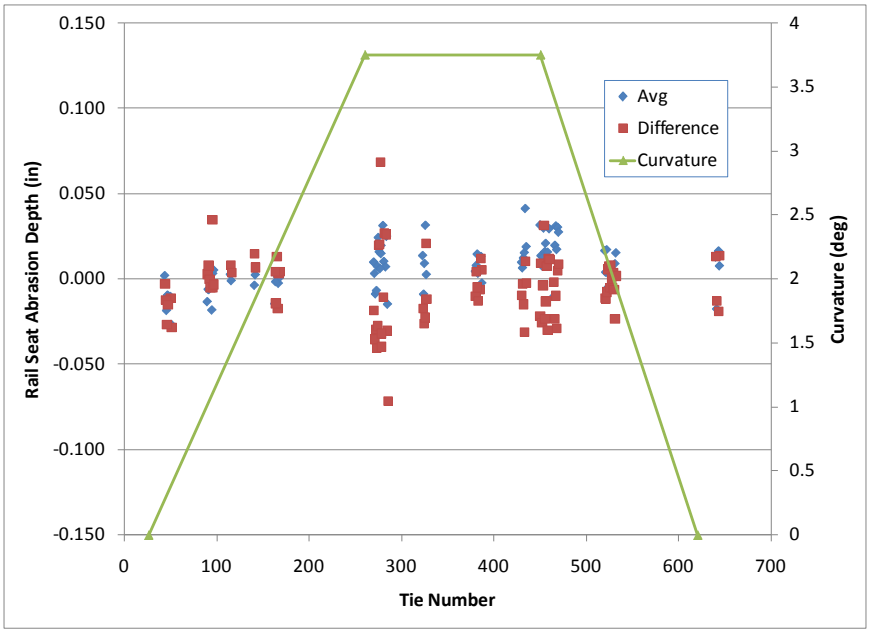

Figure 30. Low Rail MP 583 Average RSA and RSA Difference (cant)

Figure 31. MP 584.5 Typical RSA in Curve, Tie 126, and Tie 157
(Gauge side is at top of photo and shows gauge side with deeper abrasion than field side, confirming inward tilt (cant).)

The only curve that showed a significant pattern of RSA was at MP 584.5. Figure 32 shows the RSA measurements compared with track geometry measurements and NUCARS simulation results from that curve. The first graph shows the measured track curvature and superelevation/ cross level. The second graph shows the manual measurements of average RSA depth and RSA depth difference (field gauge) for the right/low rail. The third graph shows the measured track gauge and alignment and the left/high and right/low rail cants as measured by the track geometry car. The track geometry data was used as input to the NUCARS simulations.

The track geometry data data was used as input to the NUCARS simulations. The fourth and fifth graphs show the NUCARS predictions of lead axle single wheel L/V ratios and lead truck side L/V ratios, which were performed with the assumption of dry rail (rail friction coefficient of $\mu = 0.4$). In this graph, a positive L/V ratio on the right rail and a negative L/V ratio on the left rail represent gauge-spreading forces. Note that in actual practice the friction coefficients in this curve are probably different as a result of the presence of track lubricators in the vicinity, which would result in somewhat different forces and dynamic response. However, friction levels were again not measured.

Figure 33 shows the corresponding NUCARS simulation results for rail seat vertical forces and moments at the tie located at 345 ft, with Axle 1 on the left side of the graph and Axle 4 on the right. Simulations were performed at 50 and 15 mph to represent the two common operating conditions and to demonstrate the effect of speed. A wheel/rail friction coefficient of $\mu = 0.4$ was used to represent dry rail. To simplify the analyses and comparisons for this segment of the project, both the simulations were performed in the same direction, although normally the 15-mile per hour operation would be expected to be in the opposite direction.

Results show similar trends to those shown at the CSX St. Albans site: when the average force due to curvature increases, abrasion increases. No significant correlation between predicted vehicle-track forces and local track geometry features other than curvature are noticeable, and there are no areas with significantly more abrasion than is average for the curve.

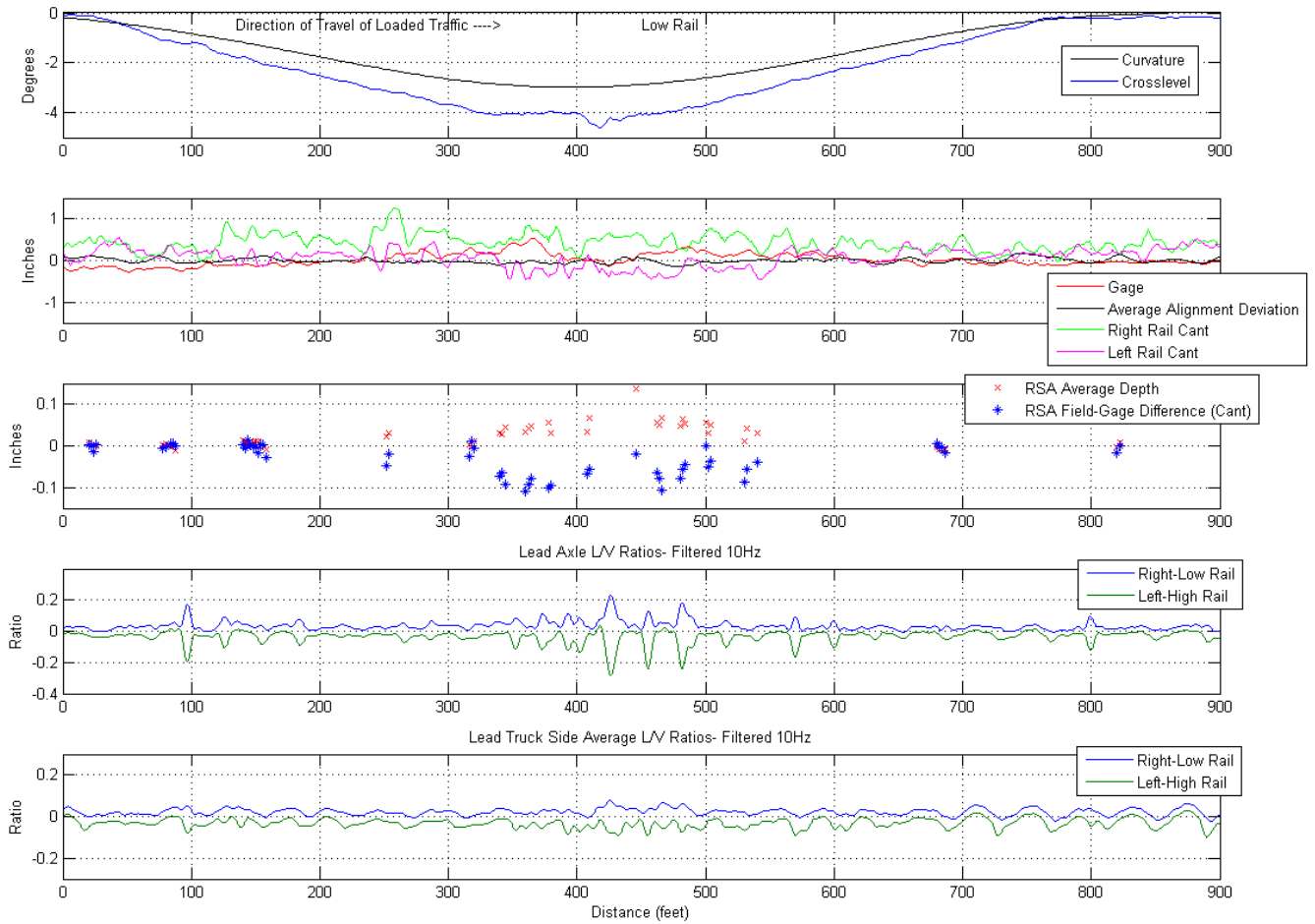

Figure 32. Curve Data for MP 584.5; Distance along Curve Measurements and Predicted Car Performance of a Loaded Hopper

(Top to bottom shows curvature and superelevation, RSA depth, track geometry data, predicted lead axle L/V ratio, and predicted lead truck side L/V ratio at 15 and 50 mph.)

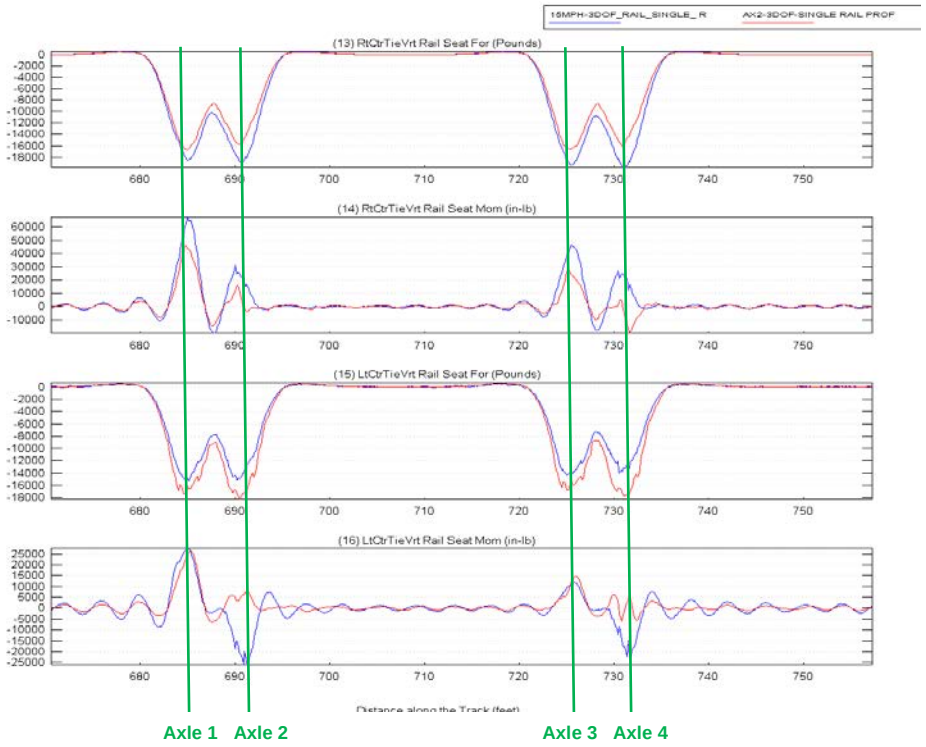

Figure 33. Rail Seat Vertical Forces and Roll Moments for MP 584.5 at Tie Located at 345 ft; Blue Lines Show Forces and Moments at 15 mph; Red Lines at 50 mph

The predicted roll moments on the low (right) rail imply forces that would tend to roll the low rail outward. This is contrary to the measured RSA patterns and track geometry car rail cant in this region of the curve, which show noticeable inward rail roll. Figure 34 and Figure 35 show the corresponding wheel/rail contact positions as well as low rail wheel and truck side L/V ratios at the tie at 345 ft for Axles 1 and 2 for the 50-mile per hour run. The gauge clearance between the wheels and rails can be seen to be somewhat less than at the St. Albans site shown in Figure 18 and Figure 19. The contact points for the wheels are shaded in red. Although both wheels are running in flange contact with the high (left) rail, Axle 2 is generating somewhat lower single wheel L/V ratios and is not pressing as hard against the flange, as demonstrated by its single point of flange contact.

The wheel/rail contact for Axle 2 is somewhat unusual, and it is probably affected by the asymmetric wear patterns of the wheel profiles used in the simulation, resulting in poor steering response. Normal expectations for a curve of this degree (2.75°) would be for the trailing axle of each truck to run closer to the center of the track without flange contact.

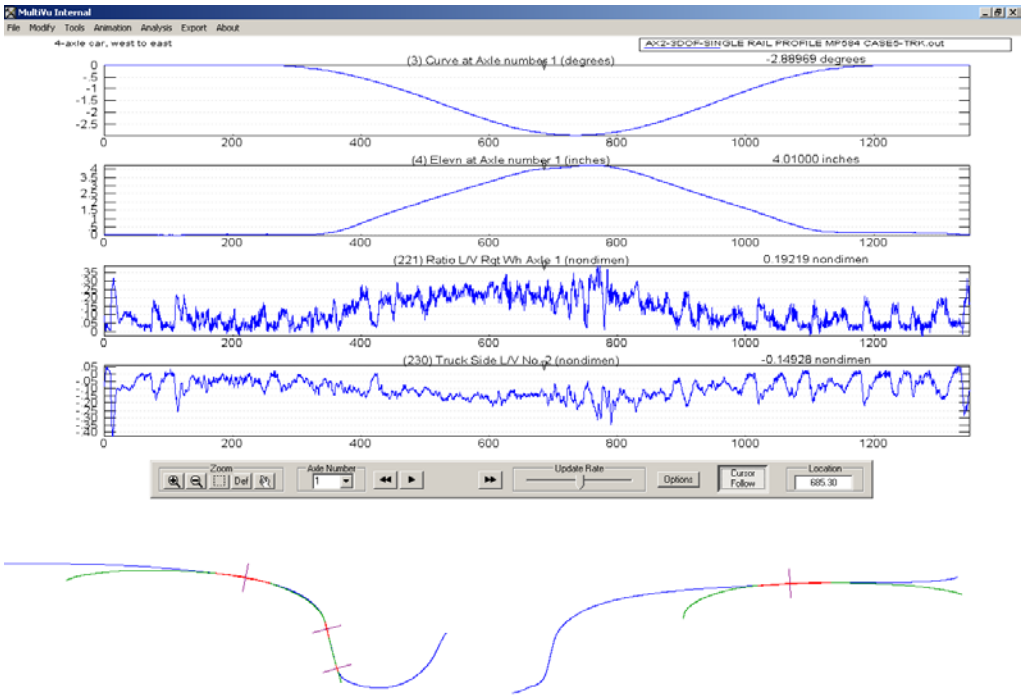

Figure 34. Wheel/Rail Contact Geometry for Axle 1 at 345 ft along the Track for MP 584.5, with Corresponding Left and Right Wheel L/V Ratios

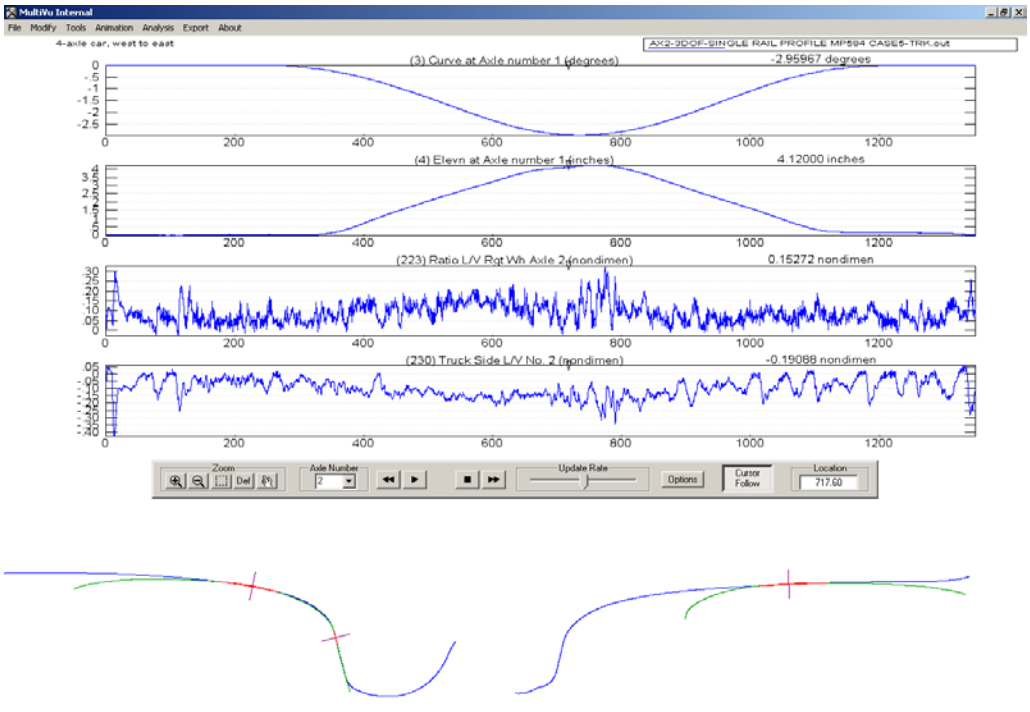

Figure 35. Wheel/Rail Contact Geometry for Axle 2 at 345 ft along the Track for MP 584.5, with Corresponding Left and Right Wheel L/V Ratios

These results clearly imply that the NUCARS simulations do not replicate the conditions present at the actual Needles site. Some possible reasons for this include the following:

- Wheel/rail friction conditions used in the model (dry rail with friction coefficient $\mu = 0.4$) are not representative of actual conditions. The friction conditions on the track were not measured at the site, although evidence of some form of lubrication was found on the gauge faces and bases the rails, and many BNSF locomotives are equipped with onboard lubricators.
- One loaded hopper car model was used for all modeling to represent a severe loading condition. However, this car model may not reflect exactly the various types of intermodal cars (including articulated cars) and mixed traffic that dominate operation at this site.
- Measured worn wheels from the CSX hopper car may not be representative of the wheels that normally run over the site.
- Track parameters (such as rail fastener and pad stiffness) used in simulation are not representative of those at the site.

The first three reasons are expected to be the most likely causes. For example, Figure 36 shows the effect on the low rail moments of simulating the following four different rail lubrication conditions:

- Dry rail ($\mu = 0.4$)
- Gauge face lubrication (top of rail $\mu = 0.35$, gauge face $\mu = 0.15$)
- Top of rail (TOR) friction modifier (top of rail $\mu = 0.4$, Kalker creep coefficients adjusted to 18 percent of nominal) [5]
- Gauge face lubrication and TOR friction modifier (top of rail $\mu = 0.35$, gauge face $\mu = 0.15$, Kalker creep coefficients adjusted to 18 percent of nominal) [5]

A considerable difference in low rail roll moments can be seen. Although none of the cases show rail moments that would tend to lead to RSA that cants the rail inward, the cases with TOR friction modifier show very low L/V ratios, and some reversal of roll moment as Axle 2 and Axle 4 pass over the tie.

The above modeling was performed with the loaded hopper car model. Although the axle loads can be similar, the truck spacing, the articulation joints, and the details of the trucks used in other cars (including intermodal cars) can sometimes result in different dynamic response. In addition, the wheel wear patterns may be different. In TTCI's experience, these differences, in combination with some of the wheel/rail lubrication conditions discussed above, could cause negative rail seat roll moments.

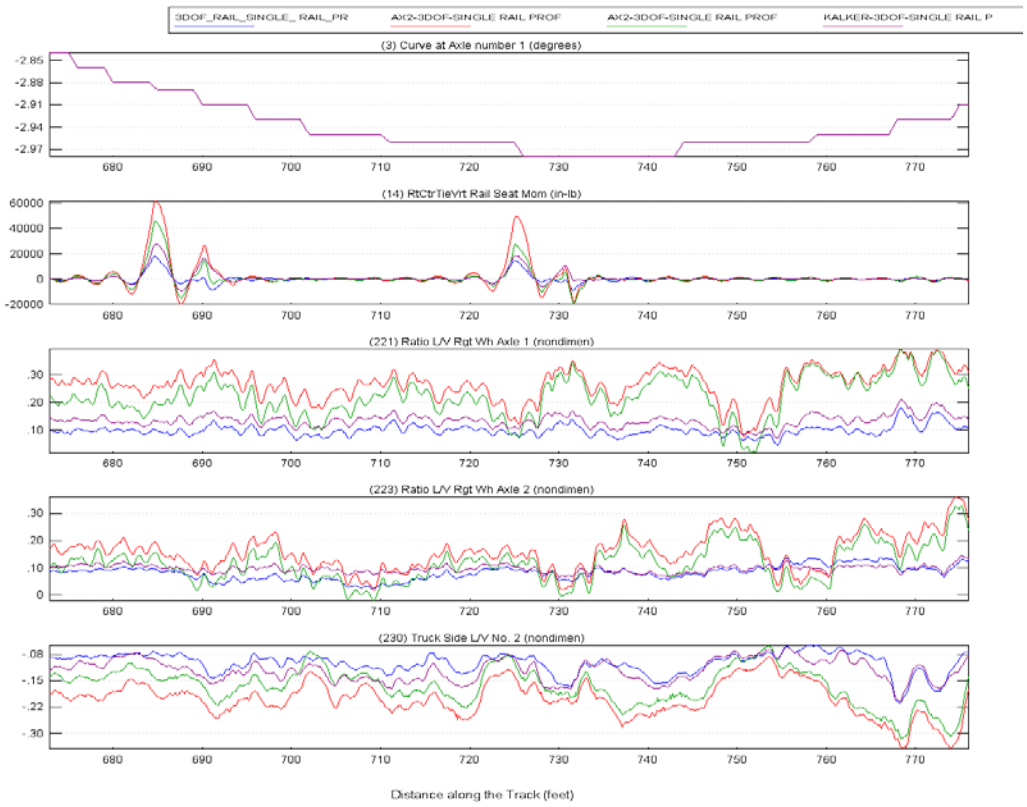

Figure 36. Effect of Rail Lubrication Conditions on Axles 1 and 2 Low Rail L/V Ratios and Low Rail Roll Moments for MP 584.5 at Tie Located at 345 ft

(Green lines show dry rails; red lines show gauge face lubrication; blue lines show TOR friction modifier; purple lines show gauge face lubrication and TOR friction modifier.)

3.3 Site 3 – BNSF near Alliance, NE

The final railroad site visited as part of this program was provided by BNSF near Alliance, NE. No preinspection trip was made for this site. Instead, part of the inspection team traveled to Alliance one day early to mark ties and measure rail profiles at the curves to be inspected over the next several days. The inspection was done the week of April 4, 2011. The location of tangent to spiral, spiral to curve, curve to spiral, and spiral to tangent was estimated for each curve, and the GPS location and tie number of key points were recorded to help when correlating the location to track geometry data. These curves are on Main 1 and carry mostly northbound traffic. The traffic is predominately unit coal trains, and it is a mix of empty and loaded trains.

Alliance has an average of 16–17 in of precipitation per year, which is a little more than Needles (10 in per year), but considerably less than St. Albans (43 in per year). Unlike the St. Albans and Needles sites, there was no visual evidence of lubrication on the rails in the vicinity.

The original inspection plan called for inspection of several fairly tight curves close to the yard in Alliance, but as the result of changes in BNSF's work schedule, the repair of these curves was postponed. Instead, some of the more shallow main line curves were repaired, and the inspection team was available to make measurements. Table 3 lists the details of the curves measured during the April 2011 work window.

Table 3. Description of Measurement Sites at Alliance, NE

Milepost (MP)	Curvature (deg)	Super-elevation (in)	Balance Speed (mph)	Normal Operating Speed (mph)	Rail Measured (high/low)	Comments, Notes, Etc.
11.8	2			50	High	
12.8	1			50	High	
22.1	1.5			50	Low	RSA previously repaired
26.1	0.5			45	Low	

Figure 37 through Figure 40 show the RSA measurements from the four curves. All of these plots use the same scales as those at the Needles site. The data shows that no severe RSA is in any of the curves measured at the Alliance site.

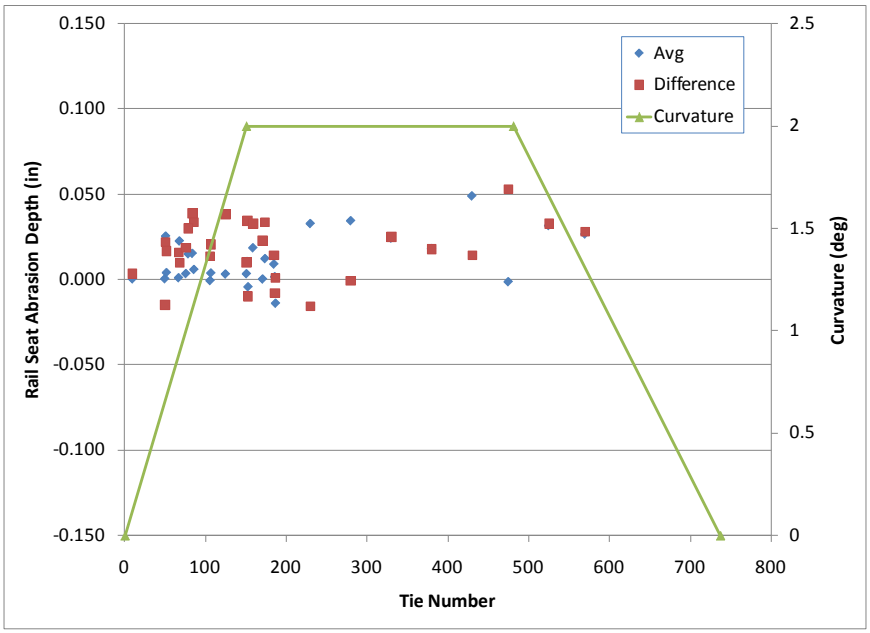

Figure 37. Curve between MP 11.9 and MP 11.6, Average RSA and RSA Cant, High Rail

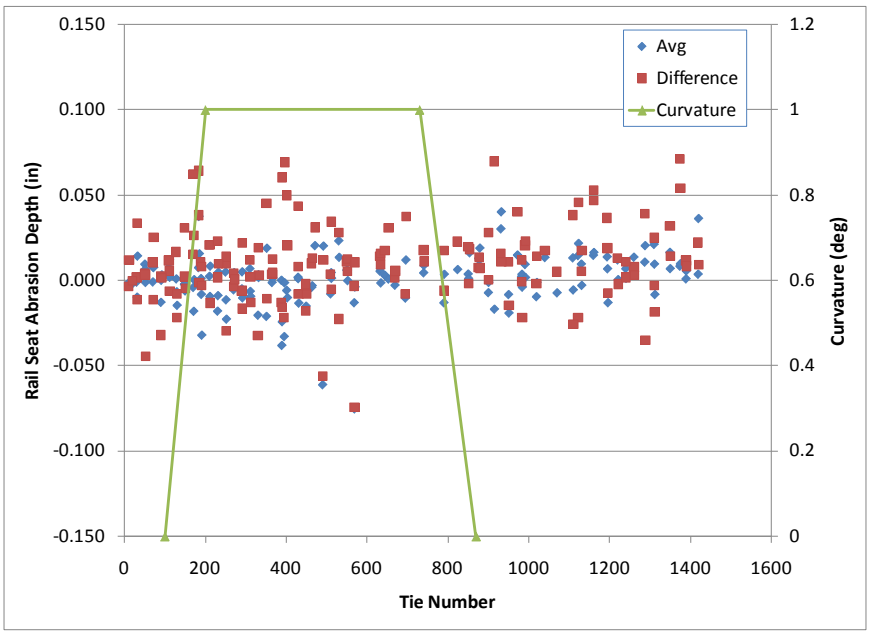

Figure 38. Alliance Curve between MP 12.96 and MP 12.62, Average RSA and RSA Cant, High Rail

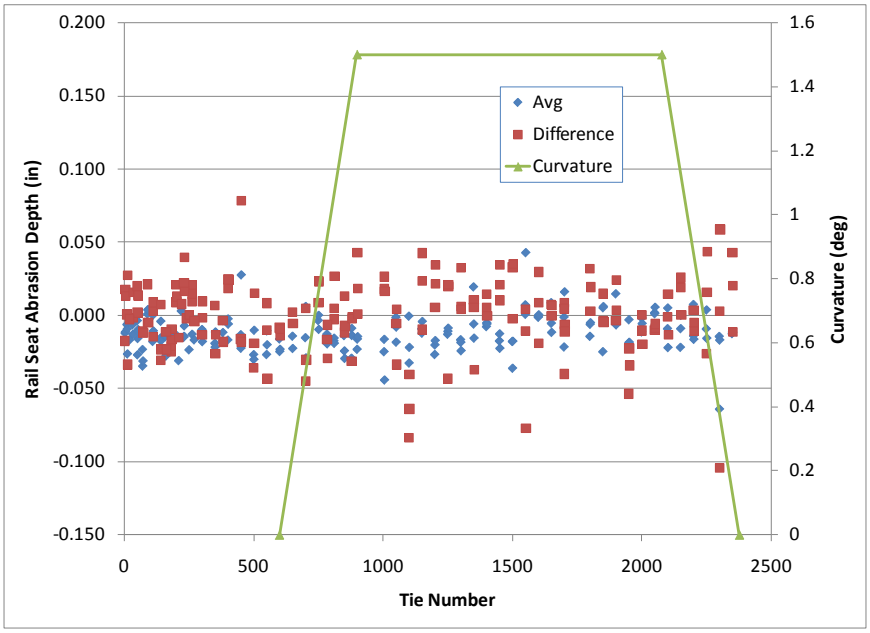

Figure 39. Alliance Curve between MP 22.6 and MP 21.7, Average RSA and RSA Cant, Low Rail

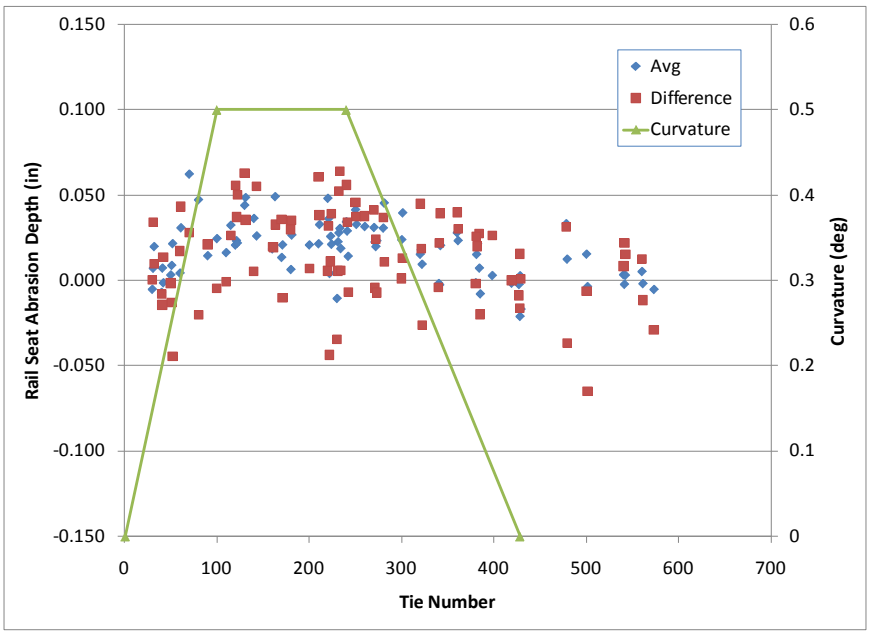

Figure 40. Alliance Curve between MP 26.3 and MP 25.95, Average RSA and RSA Cant, Low Rail

The Alliance curve at MP 12.8 seemed to have more abrasions than the other three curves measured. Good examples of abrasions are close to Tie 396. Figure 41 to Figure 43 show Ties 395, 396, and 401, respectively. Although these ties do not have deep RSA, they do show the rough texture of the onset of abrasion, especially at the field side of the rail seat.

Figure 41. High Rail Seat of Tie 395 on Curve at MP 12.8

Figure 42. High Rail Seat of Tie 396 on Curve at MP 12.8

Figure 43. High Rail Seat of Tie 401 on Curve at MP 12.8

Because little RSA was seen at the Alliance site, no NUCARS simulations were performed, and no attempt was made to correlate RSA measurements with measured track geometry.

4. Conclusions and Recommendations

4.1 Conclusions

Sixteen curves on three different railroads were inspected and analyzed for RSA. Where RSA was found, the severity appeared to be generally related to track curvature. The one inspection location with the tightest curves and the highest annual rainfall had the most RSA. Where RSA was found, the depth of the abrasion seemed to be related to the position of the tie in the curve. Areas with deep abrasion were often associated with private road crossings. In these areas, the rail seat stayed damp longer, and the rail seats were more likely contaminated with dirt or sand that could act as an abrasive. However, none of these crossings appeared to be associated with track geometry features that were likely to induce vehicle dynamic response.

The NUCARS simulations of several of the sites with RSA confirm the general correlation between RSA and track curvature. The simulations also showed that the vehicle dynamic response, wheel/rail forces, and moments generated at the rail seats are very dependent on the details of the simulation input parameters. Therefore, NUCARS simulation results did not always exactly match the measured RSA patterns. Choice of wheel profile, train speed, and wheel/rail lubrication conditions were all shown to have noticeable effects on the results. It is expected that choice of vehicles being modeled would also have similarly large effects.

A hypothesis that a particular track geometry feature (such as down-and-out perturbations) is a trigger for the development of RSA could not be confirmed from the limited number of sites where RSA was found. No large down and out perturbations were identified in the measured track geometry for any of the sites. Because of the limited number and the spacing along the track between the RSA depth measurements, it is possible that a correlation between local track geometry features and RSA could have been missed. Also, the limited number of NUCARS simulations performed by using the measured track geometry did not show any strong dynamic response to local track features that could be correlated to the RSA measurements.

Issues encountered during the inspection process that affected these outcomes include the following:

- Inspection sites were limited to locations where the host railroads were performing rail removal and replacement
- Host railroads' track maintenance plans and schedules changed at the last minute
- Requirement for the inspection team to work within very tight access windows that limited time available to make RSA measurements
- Cumbersome and slow RSA depth measurement methods

Simplifications and other issues encountered that affected the NUCARS simulation results include the following:

- Use of a single vehicle (loaded hopper car) model for all modeling
- Assumption of dry rails ($\mu = 0.4$) for the base case
- Use of single wheel profile pair for all modeling
- Track geometry data in mid chord offset format (CSX simulations)

4.2 Recommendations

An important objective could not be achieved from this segment of the project: a particular track geometry feature for installation at FAST for testing in subsequent project segments was not identified. Either more site inspections must be performed or an alternative selection method must be adopted to identify a track geometry feature.

If more site inspections are performed, an alternative method for selecting sites for inspection could be adopted, such as prescreening the measured track geometry from proposed inspection sites to determine whether the locations of large rail cants are associated with other track geometry features.

If more site inspections are performed, the following improvements in measurements are recommended:

- Develop improved, automated RSA depth gauge to permit much faster and more frequent measurements; however, the speed of measurement should not compromise the reliability and repeatability of the measurements
- To capture short wavelength effects, measure RSA more frequently, at least every other tie to permit at least five measurements in 20 ft
- Document rail lubrication conditions for each site, preferably with a tribometer to measure friction coefficients; however, most available tribometers cannot accurately measure the effects of many TOR friction modifiers [5]
- Get all track geometry measurements in space-curve format
- Measure pad thickness to estimate wear
- Measure insulator wear to estimate rail movement in rail seat
- Measure clip load to evaluate rail seat contact conditions
- Check the rail base for indications of wear or abrasion

Another alternative for selecting a perturbation to install at FAST would be to use the measured perturbation geometry from a previously inspected RSA site known to have severe perturbation geometry and/or to have contributed to derailment or other performance problems.

5. References

1. Choros, J., Marquis, B., and Coltman, M. (2007). "Prevention of Derailments due to Concrete Tie Rail Seat Deterioration," Proceedings of ASME/IEEE Join Rail & Internal Combustion Engine Spring Technical Conference, 13–16, March, Pueblo, CO
2. Reiff, R., and Gage, S. (1995). "Concrete Tie Rail Seat Abrasion Test," Proceedings of the First Annual AAR Research Review, Volume 1, FAST/HAL Test Summaries, Transportation Technology Center, Inc., 6–9 November, Pueblo, CO.
3. Reiff, R., and Gage, S. (1995 Aug.). "INTERIM Report: FAST Rail Seat Abrasion Test," *Technology Digest*, TD-95-019, Association of American Railroads, Transportation Technology Center, Inc., Pueblo, CO.
4. Cohen, A., and Hutchens, W. A. (1970). "Methods for Reconstruction of Rail Geometry from Mid-Chord Offset Data," The ASME Joint Transportation Engineering Conference, 11–14 October, Chicago, IL.
5. Fries, R., Urban, C., Wilson, N., and Witte, M. (2011). "Modeling of Friction Modifier and Lubricant Characteristics for Rail Vehicle Simulations," Proceedings of the 22nd International Symposium on the Dynamics of Vehicles on Roads and Tracks, 14–19 August, Manchester, U.K.

Abbreviations and Acronyms

COTR	Contracting Officer's Technical Representative
FAST	Facility for Accelerated Service Testing
FRA	Federal Railroad Administration
L/V	lateral/vertical ratio
MP	milepost
RSA	rail seat abrasion
TAG	technical advisory group
TTC	Transportation Technology Center (the site)
TTCI	Transportation Technology Center, Inc. (the company)
TOR	top of rail
Volpe	John A. Volpe National Transportation Systems Center